Extended IFC-based strong form meshfree collocation analysis of a bridge structure

Sang I. Park[a,b], Sang-Ho Lee[b,*], Ashkan Almasi[a], Jeong-Hoon Song[a,*]

[a] Department of Civil, Environmental and Architectural Engineering, University of Colorado, Boulder, CO 80309, USA
[b] Department of Civil and Environmental Engineering, Yonsei University, Seoul 03722, Republic of Korea

ABSTRACT

Building Information Modeling (BIM)-based finite element analysis is challenging owing to inefficiencies, such as the manual meshing/remeshing process performed by experts and excessive analysis-related information due to different input points and result nodes. To overcome these limitations, we proposed a new analysis framework that integrates the meshfree analysis method into the Industry Foundation Classes (IFC)-based bridge model. We added the IFC entities to manage information for the bridge structures and meshfree analysis based on the IFC extension concept. We developed modules for generating the bridge model based on the proposed schema. The data required for meshfree analysis were presented through the extraction and conversion process from the IFC model. Finally, the proposed framework was applied to the stress analysis of the bridge structure to demonstrate the efficiency of the method. As a result, we confirmed the possibility of seamless information exchange and interoperability between the architectural and structural analysis models.

1. Introduction

Building Information Modeling/Model (BIM), introduced to improve construction productivity and quality, has exhibited potential in various applications, such as design information management, construction simulation, virtual construction, and safety inspection. According to the Computer Integrated Construction Research Program [1], engineering analysis using BIM can reduce the cost and improve quality by finding the most effective engineering method to improve the performance of the design work via simulation during the lifecycle. In particular, Sanguinsetti et al. [2] explained that structural analysis using BIM is an important application to reduce a designer's effort. There are various commercial software packages available for the BIM-based structural analysis to achieve effective engineering advantages, such as Autodesk Robot Structural Analysis Professional [3], Trimble Tekla Structures [4], Bentley Structural Enterprise [5], and Nemetschek Allplan Bridge [6]. As stated by McGraw-Hill Construction [7], however, BIM-based structural analysis is characterized by a low level of use in the construction field. The core of this problem is due to a lack of proper interoperability and different perspectives and methods that represent the elements [8,9]. The commercial software tools also mostly generate the analysis models separately for the FE analysis, rather than directly utilize the information store in the BIM model. In addition, the linkage with the BIM management tools is not the object itself, but the ID of the objects [10]. To overcome these problems, numerous studies have described various attempts at successfully performing structural analysis using BIM [11–13]. Attempts to apply analysis using the Finite Element Method (FEM) have increased for complex and detailed components of a structural or non-linear structural analysis. Auto meshing has contributed to FEM analysis based on the BIM geometric model [14]. However, from an information exchange perspective between the information and structural analysis models these cases have several limitations: 1) additional post-processing is required to extract or regenerate information about the analytical frames from BIM objects or 2) a lack of entities for FEM-related information in the BIM model [15]. In other words, a seam may exist in the bidirectional information exchange, which drastically reduces the efficiency of the re-analytical process due to changes in the model and component replacement. This is more evident when using Industry Foundation Classes (IFC)-based information models. Many IFC viewers, including the Solibri Model Viewer [16], cannot represent analysis-related entities such as not only the *IfcStructuralAnalysisModel* but also entities connected with *IfcStructuralAnalysisModel*; even the latest official IFC (*IFC4X1*) [15] did not include FEM-related entities [15]. Therefore, we have proposed several main considerations as follows, suggesting improved processes:

* Corresponding authors.
E-mail addresses: sang.i.park@colorado.edu (S.I. Park), lee@yonsei.ac.kr (S.-H. Lee), ashkan.almasi@colorado.edu (A. Almasi), jh.song@colorado.edu (J.-H. Song).

1) Bidirectional exchange between architectural and analytical information. This requires an integrated schema that can store and manage the information contained in both models for bidirectional information exchange between the architectural and analytical models. In this study, we propose the possibility of information exchange via extension of current IFC entities.

2) Improvements in information reusability according to the re-analysis. We improve the reusability of existing acquired or newly generated information through changes in the model. The FEM must be accompanied by the remeshing process while there are changes in the shape. This leads to inefficiency as the FEM cannot reuse the existing meshes.

3) More efficient management of information regarding the inputs and results of the analysis. FE analysis is essentially an estimation method that uses variations between mesh nodes, the input/output points used for analysis should be managed separately as the locations of the input and analysis results differ. This is inefficient in terms of data management as there is an increase in the size of the analysis object.

We aim to propose an integrated information model for architectural and analytical model information, as well as to improve efficiency when managing and reusing information for re-analysis based on changes in the model. The meshfree analysis is a method that performs numerical analysis by directly using particles located in an object without the meshing process due to grid-independent, unlike the FEM. Thereby, the input particles themselves represent solution points [17–19]. In this study, we proposed the particle differential method (PDM) process as a representative meshfree analysis based on the extended IFC for the bridge structures.

2. Brief overview of BIM-based structural analysis

2.1. Structural analysis in current IFC

A key BIM feature is the efficient and accurate storage and exchange of information, as well as the reusability of information associated with its parameters. The IFC is an international open standard data schema that supports information exchange throughout the facility lifecycle [20], such that it is the core of BIM applications. IFC schema is described in the EXPRESS language as defined by ISO-TC184/SC4 [21]. IFC schema can be extended the new entities through subtyping to make it more sophisticated and specialized [22] because the EXPRESS is a complete object-oriented description language. The IFC contains basic analysis-related entities for interoperability among the structural analysis processes. We briefly reviewed the structural analysis-related entities in the IFC.

2.1.1. IFC entities for structural analysis

The Resource Layer in the IFC defines the basic resources used in other layers of it overall architecture. *IfcStructuralLoadResource* in the Resource Layer contains entities for boundary conditions, structural loads, and connections [20]. *IfcBoundaryCondition* represents the boundary conditions, and its subtypes define the details of the node, edge, and face. The analysis can be affected by action, reaction, or the loads, which can be represented by *IfcStructuralLoad* and its subtypes. Entities corresponding to a single, linear, or planar force, as well as temperature, are defined in the subtype of *IfcStructuralLoadOrResult* while IFC4 [15] supports the combination of these components by adding entities from *IfcStructuralLoadConfiguration*. Connections in *IfcStructuralLoadResource* only manage connection information for special cases, such as failure or slippage connection, and they are defined in more detail in *IfcStructuralAnalysisDomain*.

IfcStructuralAnalysisDomain, included in the Domain Layer of the IFC architecture, is defined to manage the structural engineering information [20]. *IfcStructuralAnalysisDomain* defines items that are used

directly in structural engineering, compared with the subtypes of *IfcStructuralLoadResource* that define entities at the resource level for common use across different layers. *IfcStructuralAnalysisModel* is an upper-level entity that manages assembly information related to the structural analysis model. This entity manages information in the forms of *IfcStructuralLoadGroup* and *IfcStructuralResultGroup*.

IfcStructuralAnalysisModel connects to the *IfcProject* through the *IfcRelDeclares* defined in the Core Layer. *IfcStructuralItem* and *IfcStructuralActivity* are defined as subtypes of *IfcProduct*. *IfcStructuralItem* manages information on the structural members and connections while *IfcStructuralActivity* controls information on actions and reactions. *IfcStructuralItem* and *IfcStructuralActivity* are connected through *IfcRelConnectsStructuralActivity*. *IfcRelConnectsStructuralMember* is an entity that connects structural members and structural connections, as well as supporting links with entities defined in *IfcStructuralLoadResource*.

2.1.2. IFC model view definition for supporting structural analysis

The Model View Definition (MVD) is a subset of the IFC that supports specific data exchange [23,24]; MVDs are data schemas generated by reconstructing the IFC based on the user's purposes. buildingSMART International has developed certain standards, such as the Coordination View, for design coordination among architectural, structural, and building services domains, and Reference View, for the simplified geometric and relational representation of spatial and physical components within reference model information [25]. In terms of the model applications, various MVDs have been submitted and reviewed for their applicability, such as the building energy analysis and quantity take-off [26].

In this study, we reviewed the proposal of Lehtinen and Hietanen [27,28] as well as the Structural Analysis View presented by buildingSMART International [25]. However, we focused on the proposals of Lehtinen and Hietanen in more detail because of their greater similarity to our study. Lehtinen and Hietanen presents MVDs in two manners: architectural design to structural design [28] and structural design to structural analysis [27]. This study considers both cases because our objective is to propose a method that performs a meshfree analysis based on architectural design. Lehtinen and Hietanen [28] focused on what attributes a model should generate during the structural design phase. The main purpose of this MVD is the exchange of geometric information, and it can be divided into the context, spatial element, and physical building element. *IfcProject* is the one item in the context. This model defines only basic items, such that the context can manage the project name, unit, and properties of concrete and steel materials. For the spatial elements, *IfcSite*, *IfcBuilding*, and *IfcBuildingStorey* items are selected, such that the model shows only the element name and aggregation. The only physical building elements are *IfcBeam*, *IfcColumn*, *IfcRamp*, *IfcSlab*, *IfcStair*, *IfcWall*, and *IfcBuildingElementProxy*. The model defines the element's name, classification, and association with the material. In particular, the shape representation is limited to extruded solids or boundary representations (B-reps). Lehtinen and Hietanen [27] proposed an MVD describing how to use the structural design models for structural analysis. This MVD focuses on how to use the loads, connections, and material elements among the IFC entities for structural analysis, rather than how to apply analysis elements corresponding to each entity in the IFC. In particular, this MVD defines the attributes of each entity that it should contain. This was useful when implementing the example models for verification in this study.

We extended new entities to support the meshfree analysis method; however, the existing elements were used as much as possible during the investigation based on the descriptions above.

2.2. Structural analysis in the research fields

Numerous studies have conducted a variety of investigations that

have attempted to integrate or interface BIM and structural analysis. The effectiveness of the IFC-based structural analysis is from the perspective of information exchange. Accordingly, the International Alliance for Interoperability (IAI), the predecessor of buildingSMART, has proceeded with a structural extension project related to structural analysis in the IFC2X2 version, and numerous studies have contributed to this project [29,30]. This project aimed to add entities to the IFC to integrate information related to structural analysis. The project was eventually integrated into the IFC and became an important reference for IFC-based structural analysis. Improving the applicability and supplemental schema of the IFC-based structural analysis have been significant components of recent studies.

Several studies have suggested methods for practical frame analysis via an information interface between the architectural model and the structural analysis model. Hu et al. [31] proposed a structural analysis process based on information conversion from a rule-based extraction of geometric information, such as lines and area for the B-rep-based model. Liu et al. [32] presented an information linking process between the architectural and structural models based on data conversion using a developed tool similar to the one used by Hu et al. [31]. Ramaji and Memari [12] proposed a more detailed structural analysis method, which applies separate processes by dividing the information as direct exchange units and interpretation units from the BIM data to increase the efficiency of the analysis. To stay up to date with recent studies, the structural analysis performance of BIM-IFC-based commercial software has also been improving [11]. These studies were predominantly focused on processes for architectural BIM-interpretation-frame analysis. This process has the following problems: 1) preparing the general relations related to extraction is difficult owing features that are highly dependent on changes in the shape and 2) a significant amount of manual editing is required when interpreting components such as model connections and joints. Effectively solving these problems requires further research.

FE analysis is indispensable for studying specific elements with complex shapes. In the general BIM-based FE analysis process, geometric information is directly delivered to the analysis software while non-geometric information, such as connection information and material properties, is used throughout the interpretation phase as the current IFC does not support FE analysis. Qin et al. [33] proposed a BIM-based FE analysis process using the Extensible Markup Language (XML) as a parametric file to transfer information extracted from the IFC to the commercial software. Pukl et al. [34] proposed a method to manage FEM-related elements not supported by the IFC using IFC user-defined property sets. Ninić et al. [35] developed an integrated system to connect required variables extracted from the architectural BIM to the FE analysis software using Dynamo, a visual programming tool supported by Autodesk Revit [36], the BIM authoring tool. In these studies, however, the FE analysis either did not directly use IFC data or depend on the quality of the auto meshing. This is not only inefficient in terms of the remeshing process, based on the analysis conditions or changes in the shape, but auto meshing itself is disadvantageous to an accurate analysis.

3. Integration process between the IFC-based bridge model and meshfree analysis

This study aimed to develop: 1) an extended IFC-based bridge information modeling method, 2) a process to apply the meshfree structural analysis method to the IFC-based model, and 3) a storage method for meshfree analysis-related information to the IFC Physical File (IPF) for effective reuse in the re-analysis or re-modeling process. Section 3.1 explains the theory of the meshfree analysis method applied in this study while Section 3.2 describes the IFC schema extension for the bridge structure and the meshfree analysis. Section 3.3 presents a method to map the information within the IFC schema for the applied structure and data connected to the meshfree analysis. Fig. 1 shows the

entire process of the mentioned contents.

3.1. Meshfree analysis method for the bridge information model

The stationary state stress distribution within continuum such as structural members can be expressed with the force equilibrium equation in domain Ω, the natural boundary on $\mathbf{\Gamma_t}$ and essential boundary conditions on $\mathbf{\Gamma_u}$, respectively.

$$\nabla \cdot \boldsymbol{\sigma} + \mathbf{b} = 0 \, in \ \Omega \tag{1}$$

$$\boldsymbol{\sigma} \cdot \mathbf{n} = \bar{\mathbf{t}} \, on \, \Gamma_t \tag{2}$$

$$\mathbf{u} = \bar{\mathbf{u}} \, on \, \Gamma_u \tag{3}$$

where ∇ denotes the gradient operator, $\boldsymbol{\sigma}$ is the (Cauchy) stress tensor, $\mathbf{b}$ is the body force, $\mathbf{n}$ denotes the unit outward normal vector on the boundary, $\bar{\mathbf{t}}$ is the traction vector, $\bar{\mathbf{u}}$ represents the displacement vector set along Γ_u, and $\mathbf{u}$ denotes the unknown displacement vector. Table 1 summarizes the numerical methods according to the domain integration and solution types.

There are no generalized solutions for most equations that include the differential expressions. This class of problem has been frequently analyzed with the weak form-based FEM approach. However, the FEM requires the integration of the weak form, and it has needed a cumbersome addition task such as meshing. To circumvent such difficulties, meshfree methods have been developed. More recently, a strong form-based meshfree analysis method directly solves the governing equation by discretizing the partial differential equations using a particle derivative approximation has been developed and generalized for various engineering problems for the computational efficiency and overcomes problems caused by the essential boundary conditions, e.g., generalized formalism for strong and weak discontinuities [18,37], moving interfaces [38], poly-crystalline solidification with the diffusive interface approach [39–41], inelastic materials [42], ocean circulation modeled with high order partial differential equations [43], and computational contact mechanics problems [44]. In particular, this method has the advantage of drawing the analysis results, such as displacement, stress, and strain, at the particle point compared with the general FE analysis [19].

In summary, the meshfree method is advantageous in terms of the amount of information for discretization and analysis because it neither requires mesh generation nor the remeshing process based on changes in the geometry. Moreover, unlike the weak form-based meshfree method, the strong form-based meshfree method can directly solve the governing equations such that the analysis results can be derived at the particle points.

In this study, we adopted a strong form-based meshfree analysis method to link the information model and structural analysis. Details for the particle derivative approximation can be found in the literature [45]. Eqs. (1)–(3) can be discretized with the approximated derivative operators as follows:

$$\sum_{I=1}^{N} \begin{bmatrix} L_{11I}(\mathbf{x}_J) & L_{12I}(\mathbf{x}_J) \\ L_{21I}(\mathbf{x}_J) & L_{22I}(\mathbf{x}_J) \end{bmatrix} \begin{pmatrix} u_{1I} \\ u_{2I} \end{pmatrix} = 0 \, at \mathbf{x}_J \tag{4}$$

$$\sum_{I=1}^{N} \begin{bmatrix} B_{11I}(\mathbf{x}_J) & B_{12I}(\mathbf{x}_J) \\ B_{21I}(\mathbf{x}_J) & B_{22I}(\mathbf{x}_J) \end{bmatrix} \begin{pmatrix} u_{1I} \\ u_{2I} \end{pmatrix} = \begin{pmatrix} \bar{t}_1(\mathbf{x}_J) \\ \bar{t}_2(\mathbf{x}_J) \end{pmatrix} at \mathbf{x}_J \tag{5}$$

$$\sum_{I=1}^{N} \begin{bmatrix} I_{11I}(\mathbf{x}_J) & I_{12I}(\mathbf{x}_J) \\ I_{21I}(\mathbf{x}_J) & I_{22I}(\mathbf{x}_J) \end{bmatrix} \begin{pmatrix} u_{1I} \\ u_{2I} \end{pmatrix} = \begin{pmatrix} \bar{u}_1(\mathbf{x}_J) \\ \bar{u}_2(\mathbf{x}_J) \end{pmatrix} at \mathbf{x}_J \tag{6}$$

where I are the set of neighbor nodes of the material point $\mathbf{x}_J$. $L_{ijI}(\mathbf{x}_J)$, $B_{ijI}(\mathbf{x}_J)$, and $I_{ijI}(\mathbf{x}_J)$ are the discretized differential operators associated with Eqs. (1)–(3) which are given by:

$$L_{11I}(\mathbf{x}_J) = (\lambda + 2\mu)\Phi_I^{[2,0]}(\mathbf{x}_J) + \mu\Phi_I^{[0,2]}(\mathbf{x}_J) \tag{7a}$$

$$L_{22I}(\mathbf{x}_J) = \mu\Phi_I^{[2,0]}(\mathbf{x}_J) + (\lambda + 2\mu)\Phi_I^{[0,2]}(\mathbf{x}_J) \tag{7b}$$

*: The extended or related IFC entities that represent the bridge structures
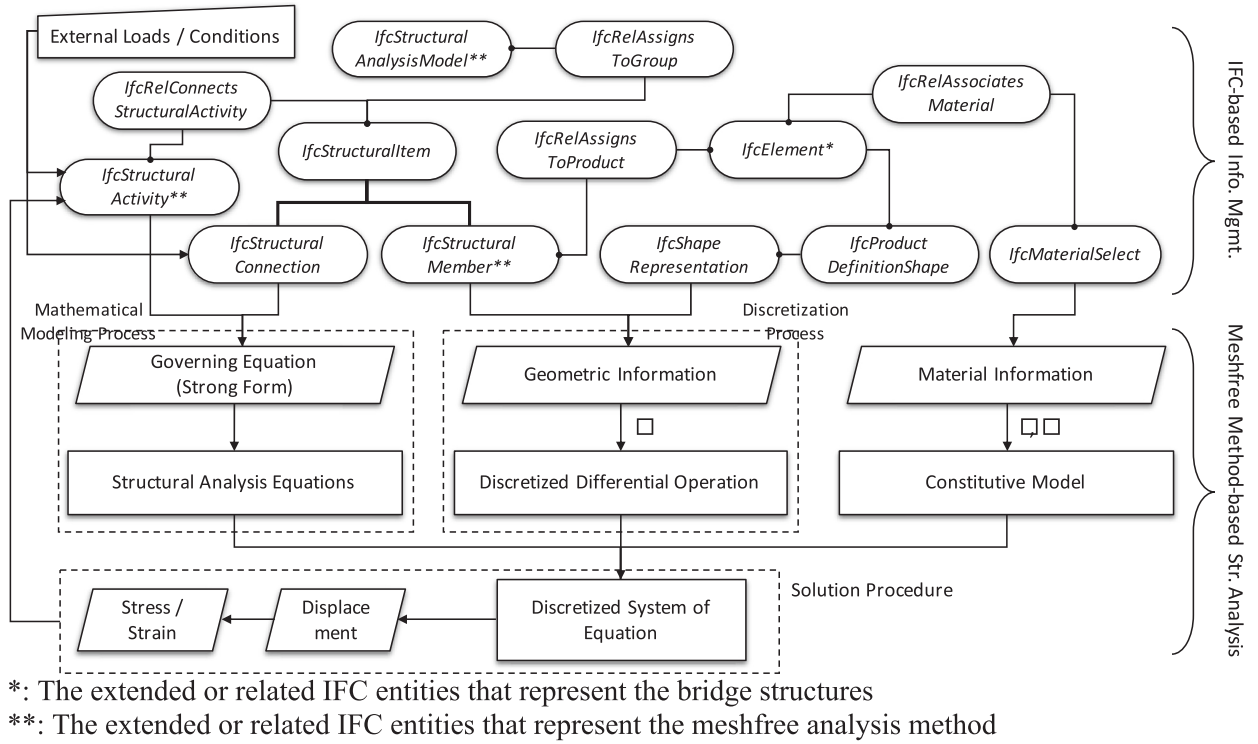**: The extended or related IFC entities that represent the meshfree analysis method

Fig. 1. Entire process for the extended IFC-based meshfree analysis method.

Table 1
A comparison of the mesh-based and meshless analysis methods.

	FEM (weak formulation)	Meshfree (weak formulation)	Meshfree collocation (strong formulation)
Connectivity	O	×	×
Domain integration	O	O	×
Solution on grid/particle point	Displacement ($\mathbf{u}$)	Displacement ($\mathbf{u}$)	Displacement ($\mathbf{u}$), stress ($\boldsymbol{\sigma}$), and strain (ε)

$$L_{12I}(\mathbf{x}_J) = L_{12I}(\mathbf{x}_J) = (\lambda + \mu)\Phi_I^{[(1,1)]}(\mathbf{x}_J) \tag{7c}$$

$$I_{11I}(\mathbf{x}_J) = I_{22I}(\mathbf{x}_J) = \Phi_I^{[(0,0)]}(\mathbf{x}_J) \tag{8a}$$

$$I_{12I}(\mathbf{x}_J) = I_{21I}(\mathbf{x}_J) = 0 \tag{8b}$$

$$B_{11I}(\mathbf{x}_J) = (\lambda + \mu)\Phi_I^{[(1,0)]}(\mathbf{x}_J)n_1 + \mu\Phi_I^{[(0,1)]}(\mathbf{x}_J)n_2 \tag{9a}$$

$$B_{22I}(\mathbf{x}_J) = \mu\Phi_I^{[(1,0)]}(\mathbf{x}_J)n_1 + (\lambda + \mu)\Phi_I^{[(0,1)]}(\mathbf{x}_J)n_2 \tag{9b}$$

$$B_{12I}(\mathbf{x}_J) = B_{21I}(\mathbf{x}_J) = \mu\Phi_I^{[(1,0)]}(\mathbf{x}_J)n_2 + \lambda\Phi_I^{[(0,1)]}(\mathbf{x}_J)n_1 \tag{9c}$$

where λ and μ are the Lamé constants, and $\Phi_I^{[\boldsymbol{\alpha}]}(\mathbf{x})$ is the generalized shape function that implies an α-order derivative approximation for node I. As a result, the strong form-based meshfree analysis method can be expressed using the shape of the objects ($\boldsymbol{\Phi}$, n) and the material information (λ, μ). For the stress analysis, the static force equilibrium condition is adopted with small strain isotropic linear elasticity model; details about the formalism can be found in the literature [18,37,41].

3.2. IFC extension to support the bridge structure information modeling and meshfree analysis method

The information set of a bridge [46,47] *BI*, can be represented as follows:

$$BI = \bigcup\{P, Q, RL\} \tag{10}$$

where *P* is a set of information that directly represents the bridge and its components, *Q* is a set of information qualifying *P*, and *RL* is a set of relations among the information objects. The set *Q* can be further categorized as follows:

$$Q = \bigcup\{E, A, B\} \tag{11}$$

where *E* is a set of environmental conditions or constraints that are generally based on natural conditions and performance requirements, such as wind velocity, geological features, peak ground acceleration, water velocity, and budget. *A* is a set of information manipulated for lifetime activities conducted for multiple purposes (environmental information and physical body information are excluded), such as design codes, i.e., load factors and limit states of bridge members, and the condition states of bridge members. *B* is the physical body information, such as the geometry and material information that describes physical elements of the bridge, i.e., the locations, lengths, material strengths, and the sectional dimensions and properties.

In the IFC kernel, the subtypes of *IfcRelationship* are *RL*, the subtypes of *IfcPropertyDefinition* are *Q*, and the subtypes of *IfcObjectDefinition* can be considered as combinations of *P* and *Q*. Elements related to structural analysis can be categorized as parts that deal with information themselves related to structural analysis (*P*), parts that manage loading and boundary conditions required to structural analysis (*A* and *B*), and parts that connect them (*RL*). We extended the elements belonging to parts of the *A* and *B* domains as much as possible, but added new entities as the parts of the P domain when expressing new objects, such as physical or spatial components of the bridge. The elements constituting the bridge structure and particles used directly for meshfree analysis have added as new entities in the part of the element object. The analysis-related information, such as load, boundary conditions, or result, was managed using current resources or new extended entities. We
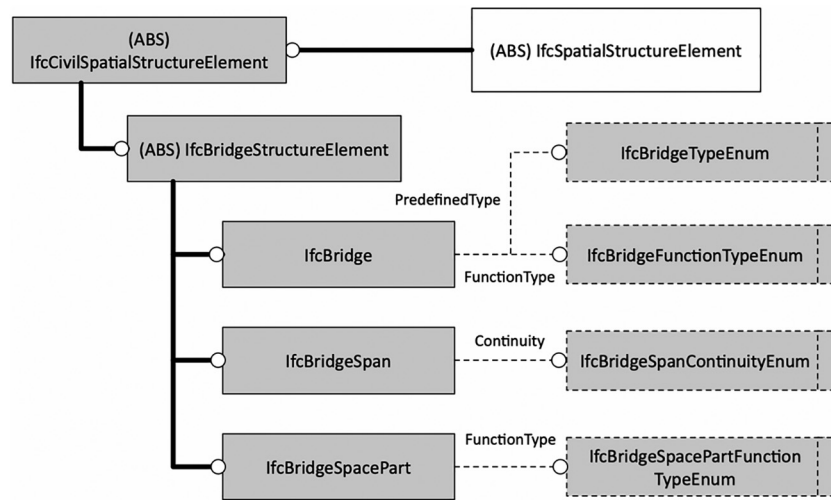
Fig. 2. EXPRESS-G diagram for the spatial structural elements of the bridge model; the shaded boxes denote extended entities for the bridge model.

have used the relational entities of the current IFC as is.

3.2.1. Proposed extensions to capture the bridge information model

Bridge structures have components with more specialized functions compared with other civil structures. Accordingly, the data schema for the bridge structures was first investigated in the civil engineering field. In this study, we proposed an IFC-based data schema for the bridge structures based on previous studies [48–50].

The main function of a bridge's spatial elements is to manage information about the space occupied by the bridge structure itself and the sub-elements it contains. This includes not only the physical components but also the void spaces generated by the components. Fig. 2 shows the EXPRESS-G diagram of the IFC for the spatial elements of the bridge structure. The extended IFC entities for the spatial elements were defined as *IfcBridge*, *IfcBridgeSpan*, and *IfcBridgeSpacePart*. The entity *IfcBridge* classifies the bridge structure itself while *IfcBridgeSpan* and *IfcBridgeSpacePart* manage the spatial information based on the bridge's along-road and traverse directions, respectively.

The *IfcBridge* is an entity that can manage information on a bridge structure and has the attributes of a *PredefinedType* and *FunctionType*. The *PredefinedType* defines the type of bridge superstructure, which can be instantiated by the *IfcBridgeTypeEnum* type. The *FunctionType* attribute can manage information on the bridge roles and can be instantiated by *IfcBridgeFunctionTypeEnum* type. The *IfcBridgeSpan* is an entity that manages the space, separated based on the along-road direction of the bridge. The *IfcBridgeSpan* is a subtype of *IfcBridgeStructureElement* and defines a *Continuity* attribute. As the *IfcBridgeSpan* itself is used to identify the spatial information for the along-road space parts, the *Continuity* attribute is intended to manage information on what function is contained in the span component. The *Continuity* attribute can be instantiated by the *IfcBridgeSpanContinuityEnum* type. The *IfcBridgeSpacePart* is an entity added to apply to the space, separated based on the bridge's road traverse direction. The *IfcBridgeSpacePart* is a subtype of the *IfcBridgeStructureElement* and defines a *FunctionType* attribute. The *FunctionType* attribute contains information on the role for the lane zone (or track) composing the bridge superstructure. The *FunctionType* attribute can be instantiated by the *IfcBridgeSpacePartFunctionTypeEnum* type.

The primary function of the physical entities of the bridge extensions is to handle information on the actual objects that compose or contain the bridge. Fig. 3 shows the EXPRESS-G diagram of the extended IFC data schema for the physical elements of the bridge proposed in this study. The extended IFC entities for the physical object of the bridge structure were classified into the girder, slab, abutment, pier part, and the detailed member components.

The *IfcBridgeElement* is located as a subtype of the *IfcCivilElement*. The *IfcBridgeElement* contains the *IfcBridgeGirder*, *IfcBridgeMember*, *IfcBridgeSlab*, *IfcBridgeSlabSegment*, *IfcBridgeAbutment*, *IfcBridgeAbutmentSegment*, *IfcBridgePier*, and *IfcBridgePierSegment* as subtypes. The *IfcBridgeElement* was defined as an abstract type entity that does not appear in the IPF to manage the logical hierarchy. The *IfcBridgeGirder* was added to manage girder object information for the bridge superstructure. This is a subtype of the *IfcBridgeElement* and has *PredefinedType* and *Segments* attributes. The *PredefinedType* denotes the structural girder type, such as the 'concrete box girder' or 'steel I type girder,' which can be instantiated by the *IfcBridgeGirderTypeEnum*. The *Segments* attribute was defined to control the detailed element of the girder object. A set of *IfcBridgeMember* entities can instantiate the *Segments* attribute. The *IfcBridgeSlab*, *IfcBridgeAbutment*, and *IfcBridgePier*, similar to *IfcBridgeGirder*, manage information on the slab, abutment, and pier objects, respectively. The *IfcBridgeSlab* has *PredefinedType*, *FunctionType*, and *Segments* attributes while *IfcBridgeAbutment* and *IfcBridgePier* include the *PredefinedType* and *Segments* attributes. The *PredefinedType* and *Segments* have the same role as the *IfcBridgeGirder* attributes. The *FunctionType* attribute of the *IfcBridgeSlab* can identify whether to use the general or approach type slab. Bridge components have identical geometric modeling processes, except for the functional meaning of the element. The *IfcBridgeMember* can be used for general bridge members by a single entity or several sets of entities. The *IfcBridgeMember* is a subtype of *IfcBridgeElement* and has a *PredefinedType* attribute. The *PredefinedType* of the *IfcBridgeMember* can be instantiated by the *IfcBridgeMemberTypeEnum*, which represents a functional meaning of the bridge member. The *IfcElementComponent* is an entity that was mainly to manage minor items typically not of interest with respect to the overall structural viewpoint [51]. In this study, therefore, we defined *IfcCivilElementPart* as a subtype of *IfcElementComponent* and added both *IfcBridgeElementPart* and *IfcCivilMemberConnector* as subtypes of *IfcCivilElementPart* to manage small components, such as connectors, flanges, and stiffeners used in the bridge structures. We added the *IfcCivilSharedFacility* entity to manage the shared small components that play an important structural role, such as joints and supporters, which can be controlled by the newly defined *IfcCivilJoint* and *IfcCivilBearingSupport* entities. The detailed attributes they contain are not directly related to the purpose of this study and are, therefore, not discussed.

3.2.2. Proposed extensions to capture meshfree analysis information

Here, we describe the extended IFC entities for the BIM-based meshfree analysis method. The extended schema consists of two parts, i.e., the meshfree analysis element and the structural activity.

The *IfcStructuralMember* is the superclass of all the structural items that represent the idealized structural behavior for the facility elements;
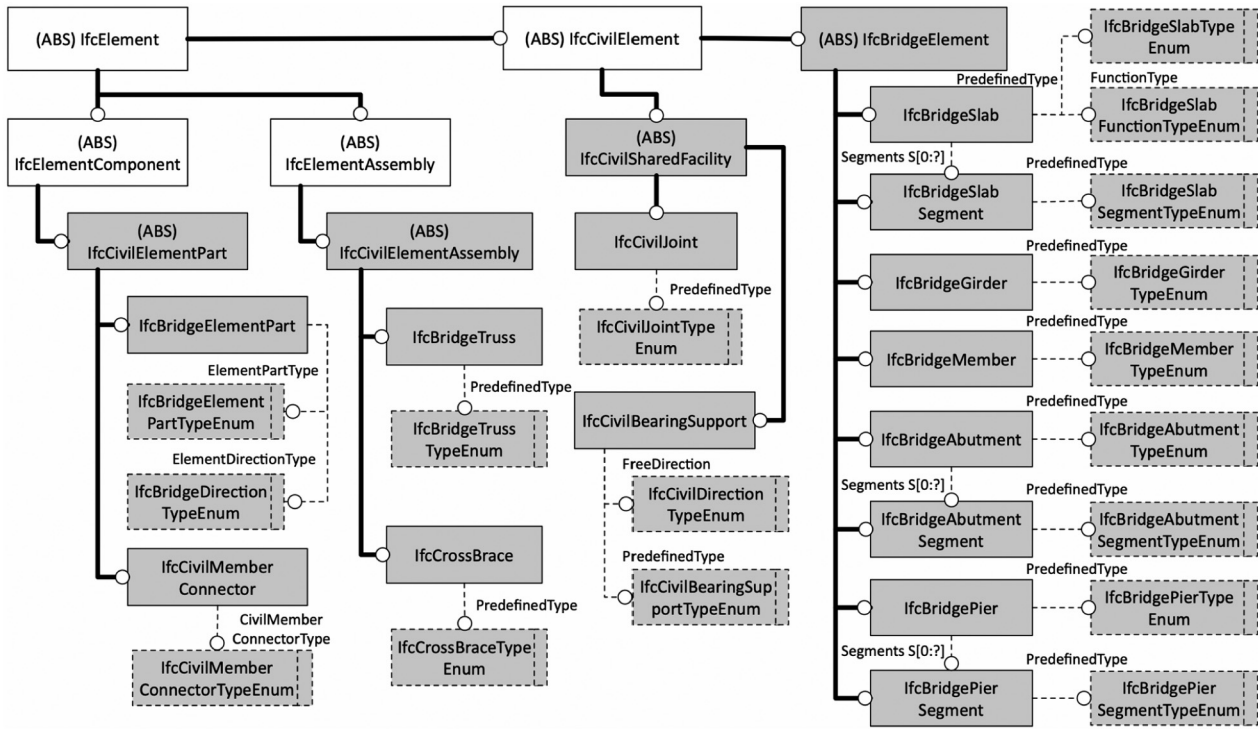
Fig. 3. EXPRESS-G diagram for the physical elements of the bridge model; the shaded boxes denote extended entities for the bridge model.

it includes the *IfcStructuralCurveMember* and *IfcStructuralSurfaceMember* as subtypes. This class only handles curves or surface members as structural objects. Since the meshfree analysis particles can be used as structural analysis objects (as explained in Section 3.1), we added an entity of *IfcStructuralPointMember* and set it as a subtype of *Ifc-StructuralMember*. The *IfcStructuralPointMember* defines the *Pre-definedType* and *PointDir* attributes, where *PointDir* can be instantiated by the *IfcDirection* entity and represents information on the direction of the particle point. These attributes can be connected with the external load (*LoadedBy* attribute) and analysis result (*HasResults* attribute) through the *IfcStructuralAnalysisModel* as the *IfcStructuralPointMember* was set as a subtype of the *IfcStructuralMember*. The *IfcStructur-alResultGroup* that implements the *HasResults* attribute, however, cannot represent information about the analysis method. The *Analy-sisMethod*, therefore, was added as an attribute of *IfcStructur-alResultGroup*, such that we can manage this as instantiating by *IfcA-nalysisMethodTypeEnum* type. The following represents the EXPRESS of the *IfcAnalysisMethodTypeEnum*:

analysis information at the particle point. The meshfree method, there-fore, has the advantage of managing the direct results of the stress and strain, as well as the displacement, which can be effectively reused during the re-analysis process based on the changes in the shape of the model. Therefore, we added the *IfcStructuralSingleStress* and *IfcStructur-alSingleStrain* entities with attributes of the XX, XY, XZ, YX, YY, YZ, ZX, ZY, and ZZ directions to manage the result information. Fig. 4 shows the EXPRESS-G diagram for the IFC extension to support the meshfree ana-lysis.

3.3. Information mapping between the bridge structure and meshfree analysis models

3.3.1. Data extraction from the bridge information model

Analysis particles used directly in the meshfree analysis can be ex-tracted and converted based on the geometry of the information model. Fig. 5 shows the process of extracting the boundaries of an area element from IFC model objects that are generated using the general extruded

TYPE IfcAnalysisMethodTypeEnum = ENUMERATION OF

(FRAME_ANALYSIS_METHOD, FEM_ANALYSIS_METHOD,

MESHFREE_ANALYSIS_METHOD, XFEM_ANALYSIS_METHOD, USERDEFINED,

NOTDEFINED);

END_TYPE;

The *IfcStructuralActivity* that manages the items for the structural actions or reactions deals with the loaded forces through the *AppliedLoad* attribute and is represented through the *IfcStructuralLoad* entity. The instances for the load are represented by the subtypes of the *IfcStructuralLoadStatic* entity that is set as the subtype of the *IfcStructuralLoad*. In IFC4, the *IfcStructuralLoadStatic* includes the *IfcStructuralLoadLinearForce*, *IfcStructuralLoadPlanarForce*, - *IfcStructuralLoadSingleDisplacement*, *IfcStructuralLoadSingleForce*, and - *IfcStructuralLoadTemperature* as the subtypes. As described in Section 3.1, unlike the FEM mesh, the meshfree analysis method can manage all

solid.

The *IfcElement* in Fig. 5 is the superclass that represents the physical objects in the IFC and includes all of the extended entities for the bridge structures proposed in Section 3.2.1. *ObjectPlacement*, an attribute of *IfcElement*, contains the axis placement information for the model object generated in a local or relative coordinate system. The transformation matrix can be created based on the values of the ①s in Fig. 5. The physical objects are represented with *IfcExtrudedAreaSolid*. The ②s in Fig. 5 indicate the position of the object (*Position*) to be represented, the direction for extrusion of the 2D profile into a 3D (*ExtrudedDirection*),
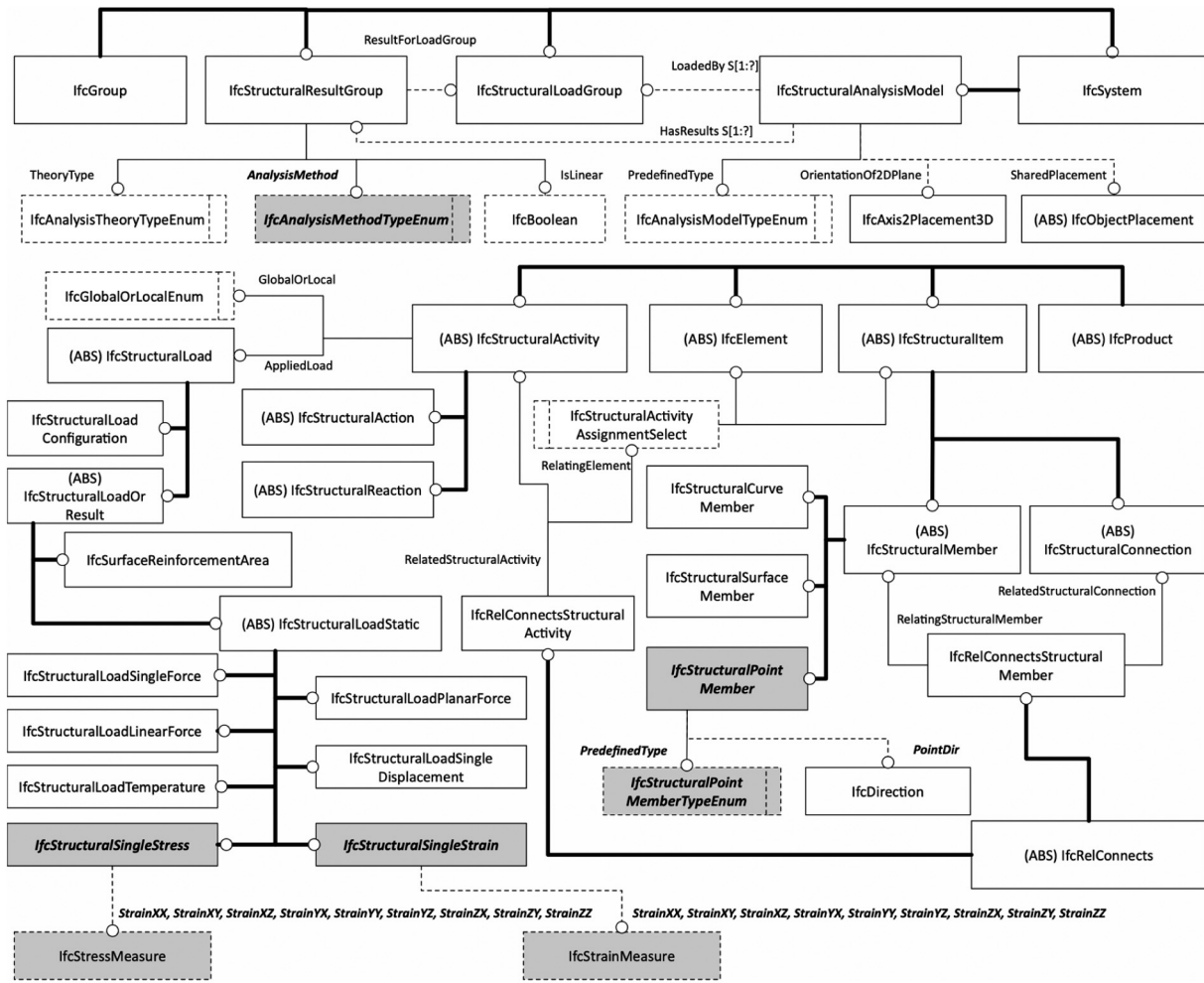
Fig. 4. EXPRESS-G diagram to support the meshfree analysis method; the shaded boxes denote extended entities for meshfree analysis.

and its length (*Depth*). The 2D profile is managed by the *SweptArea* attribute in *IfcExtrudedAreaSolid*. An arbitrary shape object, including an internal void, can be represented by *IfcArbitraryProfileDefWithVoids*. This entity manages information for the vertices as a series of points, and has *OuterCurve* and *InnerCurves* attributes that control both the outer and the inner empty boundary. These attributes use subtypes of the *IfcCurve*, such as straight lines, curves, or a combination of these. When the profile is generated through a combination of curves, it can be controlled through the *IfcCompositeCurve* as shown in Fig. 5, where each part is managed in *IfcCompositeCurveSegment*. Therefore, the final values for the profile information are the instances of the *IfcCompositeCurveSegment* entity, such that these are the vertices or shape parameters that constitute the boundary of the geometric object.

Assuming that the information is correctly delivered to the IFC during model generation, the material property for analysis has a relatively simple structure. This material can be classified into a case for managing the property based on the name of the material or a case that specifies the features through the IFC user-defined property set. Fig. 6 shows the extraction process of the material property used in this study.

In general, the material properties applied to the IFC model can be extracted through the *IfcMaterial* (shown as ① in Fig. 6). More specific data can be stored through the subtypes of the *IfcProperty* represented by the *IfcPropertySingleValue* as shown by ②s in Fig. 6, which are managed through the *IfcMaterialProperties*. The *IfcMaterial* is connected to the subtype of the *IfcElement* through the *IfcRelAssociatesMaterial*.

3.3.2. Integration of the analysis data with the IFC-based bridge model

The results of the meshfree structural analysis can be directly computed based on the location and direction vectors of the particles in the computational domain as described in Section 3.1. The *IfcStructuralPointMember* entity can manage the particle-related information (in Fig. 7, the IFC extended entities for meshfree analysis were denoted by an asterisk*). In the *IfcStructuralPointMember* entity, the meshfree analysis particles can be managed with a *Representation* attribute that is instantiated by the *VertexGeometry* attribute of the *IfcVertexPoint* that is connected with the *IfcProductDefinitionShape* and *IfcTopologyRepresentation* entities (① in Fig. 7). The direction vector of an analysis particle can be represented by the *PointDir* attribute of the *IfcStructuralPointMember*. The *PointDir* can be instantiated by the *IfcDirection* entity (② in Fig. 7). When the analysis particles require visualization by the commercial tools, they may be replaced by the *IfcStructuralPointConnection* entity. In this case, however, the analysis particles are unable to indicate direction information on the particles.

The analyzed results based on the meshfree analysis method consist of the displacement at the particles, as listed in Table 1. Therefore, the geometric change in the model shape after analysis can be directly tracked by combining the geometric changes with the particle location information before particle analysis managed by the *IfcStructuralPointMember* entity. This is one of the efficiencies of the proposed method. In this study, the particles after the analysis can also be managed by the *IfcStructuralPointMember* entity, which can then be used as input information for the re-analysis process. Instances of *IfcStructuralPointMember* containing particle information can be integrated
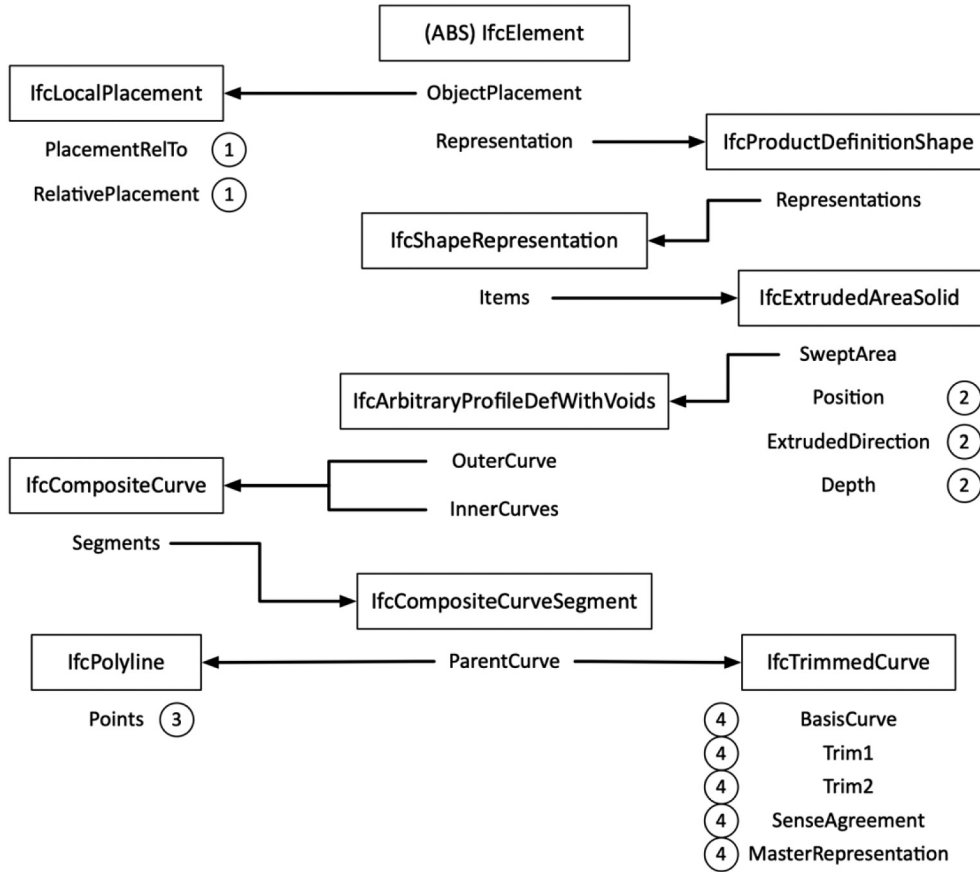
Fig. 5. Extraction of the geometric representation data for the physical elements.
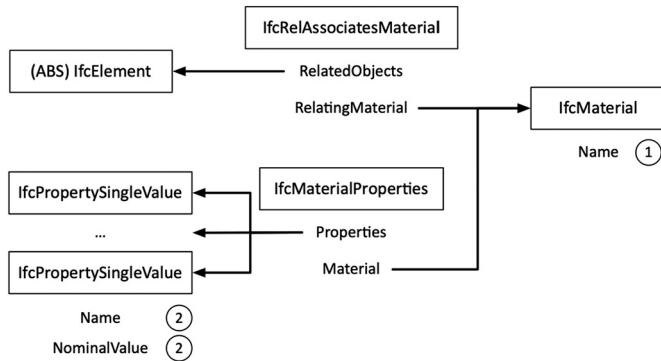

Fig. 6. Extraction of the material properties of the bridge model.

with analysis models represented through the *IfcStructuralAnalysisModel* entity that manages information on the entire analysis model via connections through the *RelatedObjects* attributes of the *IfcRelAssignsToGroup*. In addition, connections between the *IfcElement*, which represents a physical object, and the *IfcStructuralPointMember* can be constructed made through the *RelatedObjects* attribute of the *IfcRelAssignsToProduct* entity.

The *IfcStructuralPointAction* controls the information management of the external force required for analysis, where the reaction force information based on analysis can be managed in the subtypes of the *IfcStructuralPointReaction*. Both the *IfcStructuralPointAction* and *IfcStructuralPointReaction* are represented as instances of the *RelatedStructuralActivity* attribute of *IfcRelConnectsStructuralActivity*, which are associated with the *IfcStructuralPointMember*, i.e., an instance of the *RelatingElement* attribute. Here, *IfcStructuralPointMember* is the same entity as shown in Fig. 7. Both *IfcStructuralPointAction* and

IfcStructuralPointReaction are subtypes of *IfcStructuralActivity*, with the same attributes except for the *DestabilizingLoad* attribute that is only found in *IfcStructuralPointAction*. Forces loaded directly onto the object are managed by an instance of the *AppliedLoad* attribute as shown in Fig. 8. In this study, action/reaction occurs at a meshfree particle point; therefore, we used only the elements for single displacement, single force, temperature, single stress, and single strain applicable to the point.

4. IFC-based bridge information modeling and meshfree analysis data management

4.1. IfcBridgeAddMeshfree-based bridge information modeling with meshfree analytical information

An essential consideration for information modeling based on the architecture of the IFC is the generation of relational information between spatial and physical objects, such that the critical consideration in terms of the *IfcBridgeAddMeshfree* proposed in this study is the seamless connection between the analysis objects and the I/O information related to the meshfree analysis. Accordingly, we developed an export module that can generate an extended IFC-based information model within an integrated modeling environment to support the previously mentioned requirements. The module export process consisted of three components: 1) extraction of the geometric information, attributes, and properties, as well as obtaining the transformation information for object placement, 2) generation of an external reference file to manage the extracted and obtained information, 3) generation of an extended IFC-based IPF using the external reference file (Fig. 9).

The external reference file included the object identifiers, geometric information, and the related attributes of the bridge information model
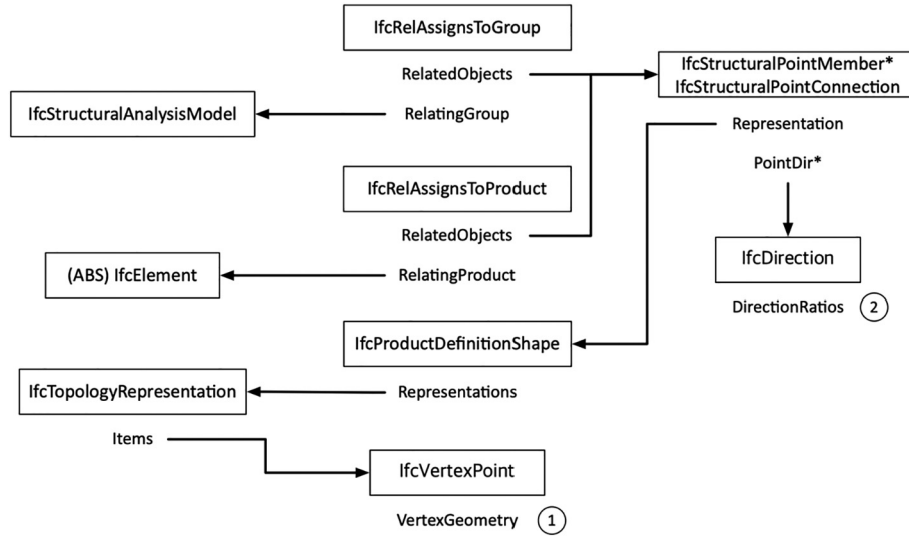
Fig. 7. Integration of the meshfree particles information with the bridge information model.
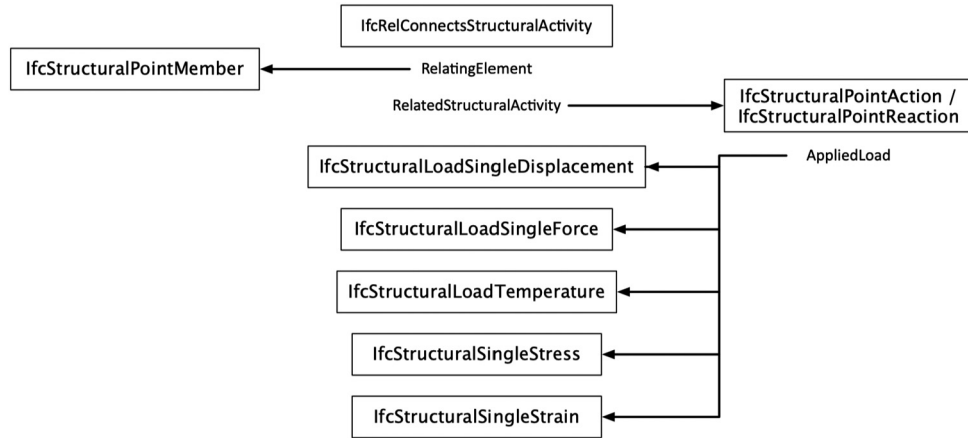

Fig. 8. Integration of the action/reaction information with the bridge information model.

extracted through the Application Programming Interface (API) within the Autodesk Revit environment. The external reference file was an XML format that included hierarchical information on the model objects. The elements of the XML file were created based on the information model elements, which contained the hierarchical information for the element, attributes of the element, and properties of the object, as well as information on the appropriate IFC entity name for use when generating the IPF file. The appropriate IFC entity was
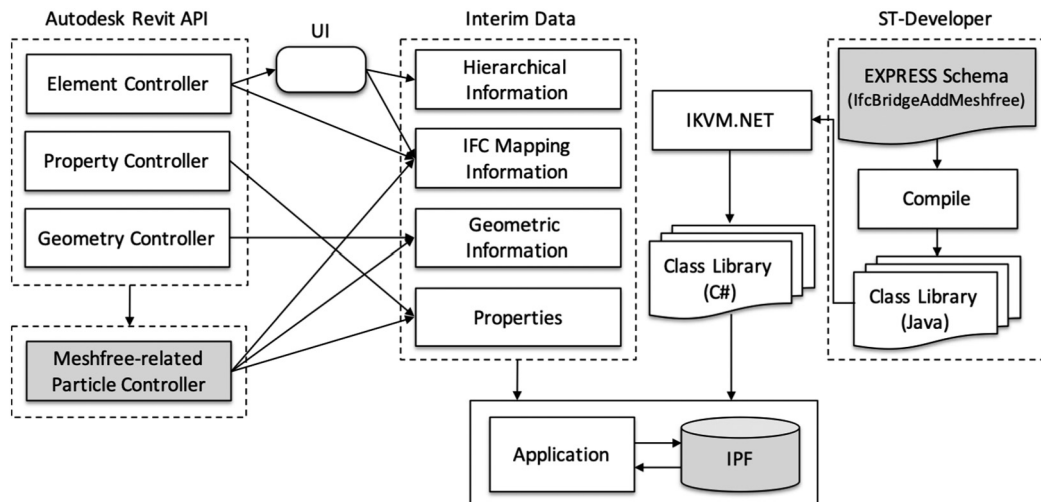

Fig. 9. Extended IFC-based (*IfcBridgeAddMeshfree*) information modeling process of a bridge structure using the BIM authoring tool.
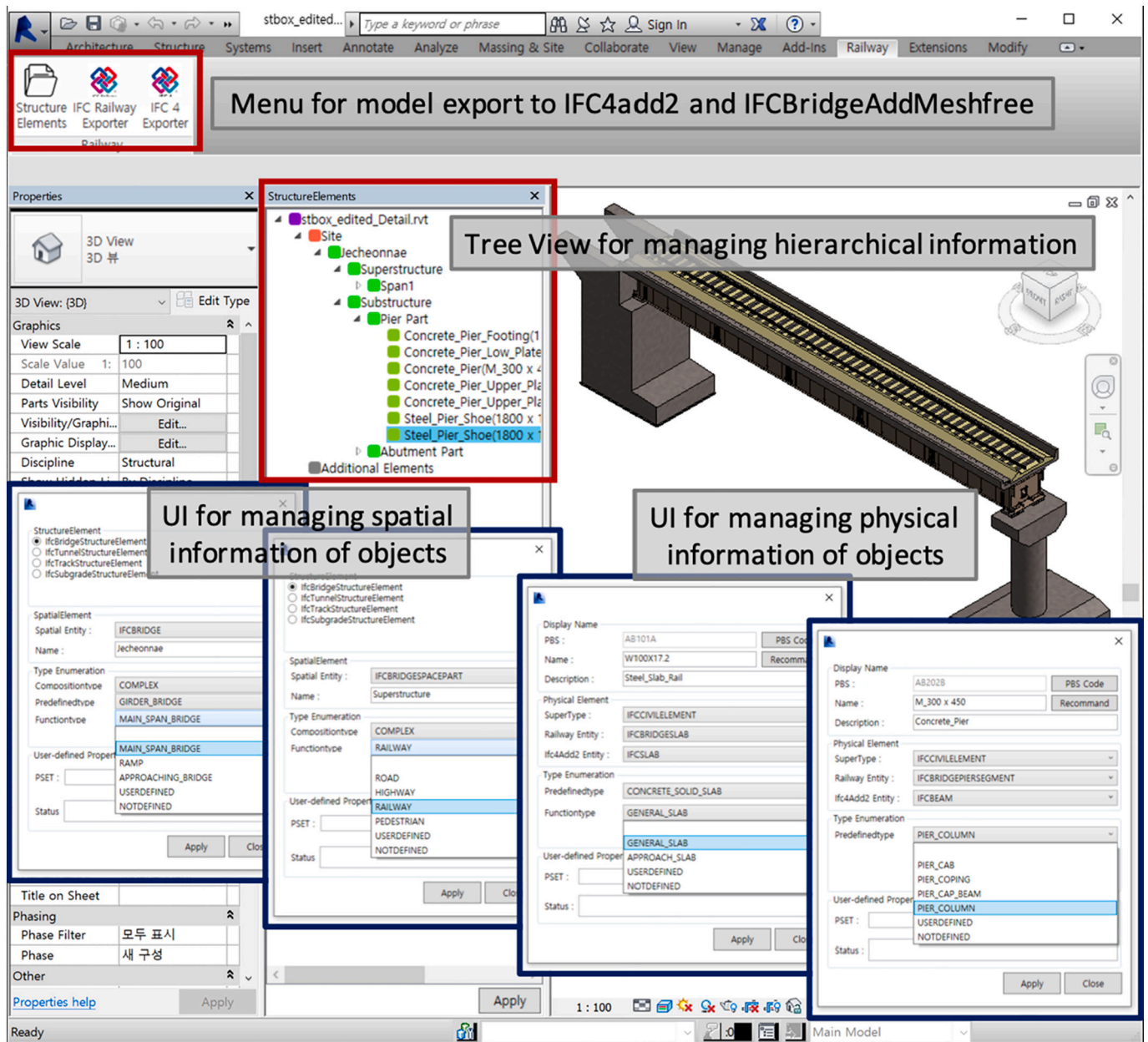
Fig. 10. User interface to manage the spatial, physical, and hierarchical information about the model.

selected using two methods: 1) automatic mapping using the attributes (classification number) included in the model object or 2) manual section by the end-user with the user-interface (see Fig. 10). The IFC representation of the geometric model was based on the tessellation of the solid objects using the identifiers of the faces and related geometric information from the vertices that compose the faces. In the case of an object modeled through the extruded area solid, the most commonly used method for generating a 3D object, the IFC representation of the object was based on the parameters of the cross-sectional profile, extrusion direction, and extrusion length. The IPF export module was developed through class libraries compiled using the ST-Developer of STEP Tools [52]. The EXPRESS code of the extended IFC schema was used to generate Java class libraries with the ST-Developer, and then the Java class libraries were converted to C# class libraries through the IKVM.NET compiler [53] to integrate the Revit API environment. The input file used to generate the IPF is an external reference file created in the previous process, such that one element of the external reference file was created as one entity of the extended IFC. The relationship between the IFC entities was based on the hierarchical information in the external reference file. The association between a spatial entity and another spatial entity located in the same hierarchy was used as the *IfcRelAggregates* entity, such that the connection between the spatial entity and physical elements contained in the spatial entity was used as the *IfcRelContainedInSpatialStructure* entity. The spatial or physical elements were linked to the property entities using the *IfcRelDefinesByProperties* entity. To create visualizations using the IFC4-based commercial tools, this module also generated IFC4-based IPF that represented physical entities as the *IfcBuildingElementProxy* entities.

4.2. Information management for use in the meshfree analysis process

4.2.1. Generation of input data from the IPF for meshfree analysis application

According to Eqs. (7)–(9), the meshfree analysis required primary particles, domain information of the particles, normal vectors of the particles in the boundary regions, and material properties, as well as the
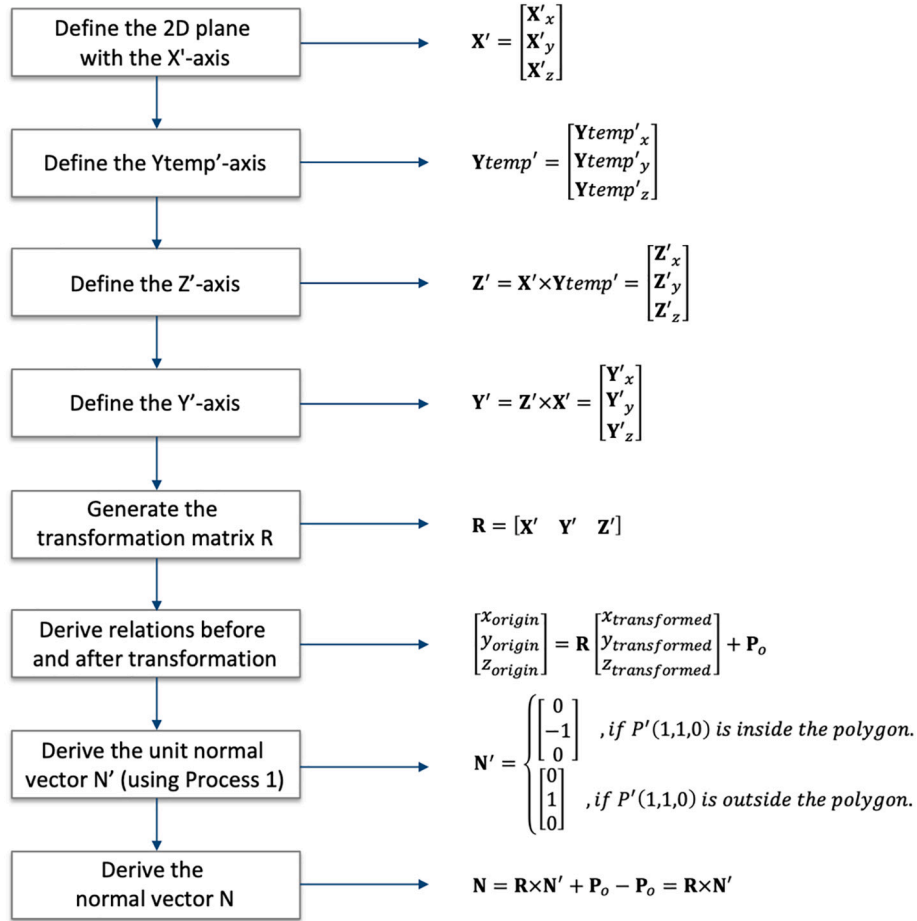
| Define the 2D plane with the X'-axis | $\mathbf{X'} = \begin{bmatrix} \mathbf{X'}_x \\ \mathbf{X'}_y \\ \mathbf{X'}_z \end{bmatrix}$ |

$$\mathbf{X'} = \begin{bmatrix} \mathbf{X'}_x \\ \mathbf{X'}_y \\ \mathbf{X'}_z \end{bmatrix}$$

Define the Ytemp'-axis

$$\mathbf{Y}temp' = \begin{bmatrix} \mathbf{Y}temp'_x \\ \mathbf{Y}temp'_y \\ \mathbf{Y}temp'_z \end{bmatrix}$$

Define the Z'-axis

$$\mathbf{Z'} = \mathbf{X'} \times \mathbf{Y}temp' = \begin{bmatrix} \mathbf{Z'}_x \\ \mathbf{Z'}_y \\ \mathbf{Z'}_z \end{bmatrix}$$

Define the Y'-axis

$$\mathbf{Y'} = \mathbf{Z'} \times \mathbf{X'} = \begin{bmatrix} \mathbf{Y'}_x \\ \mathbf{Y'}_y \\ \mathbf{Y'}_z \end{bmatrix}$$

Generate the transformation matrix R

$$\mathbf{R} = \begin{bmatrix} \mathbf{X'} & \mathbf{Y'} & \mathbf{Z'} \end{bmatrix}$$

Derive relations before and after transformation

$$\begin{bmatrix} x_{origin} \\ y_{origin} \\ z_{origin} \end{bmatrix} = \mathbf{R} \begin{bmatrix} x_{transformed} \\ y_{transformed} \\ z_{transformed} \end{bmatrix} + \mathbf{P}_o$$

Derive the unit normal vector N' (using Process 1)

$$\mathbf{N'} = \begin{cases} \begin{bmatrix} 0 \\ -1 \\ 0 \end{bmatrix} , if\ P'(1,1,0)\ is\ inside\ the\ polygon. \\ \begin{bmatrix} 0 \\ 1 \\ 0 \end{bmatrix} , if\ P'(1,1,0)\ is\ outside\ the\ polygon. \end{cases}$$

Derive the normal vector N

$$\mathbf{N} = \mathbf{R} \times \mathbf{N'} + \mathbf{P}_o - \mathbf{P}_o = \mathbf{R} \times \mathbf{N'}$$

Fig. 11. Derivation process of the normal vector for a particle located on the polygon.

external loading and boundary conditions. It is appropriate that the particles are scattered arbitrarily from the general application of the meshfree analysis method. In this study, however, the particles requiring normal vectors located on the boundary and particles located inside the object domain were generated using the separation process for an efficient computing cost. We extracted the vertices of each object from the IPF and used them to generate particles on the boundary region. Particles were created at equal intervals between the vertices for straight edge lines. In the case of part of the circumference of a circle (an arc), particles were generated by arithmetic calculations using parameters that compose the vertices and curves. Particles located inside the domain were randomly generated by using the position of the outermost box (bounding box). At that time, the generated particles did not have any additional information other than the coordinates of the position. Through an additional process, we derived the domain locations of the particles and normal vectors. This allowed us is to enable the meshfree analysis based on the information model of any particle independent of the particle generator.

The domain judgment process of the generated particles consisted of determining a point inclusion in a polygon and deriving the domain where the particles are located by combining the results of the first processes. To determine the inclusion of a point in a polygon, we referred to "The Cross Number (CN) Method," an algorithm proposed by Akenine-Möller et al. [54] and Sunday [55]. We also applied a new process to identify particles located on the boundary. The CN method counts the number of times the particles cross the boundary edges of the polygon using a horizontal line starting from a point P. In the CN method, point P is outside of the polygon if the cross number was even. Otherwise, point P is inside. To implement this algorithm, we

performed the following processes (Process 1):

i) The y-coordinate of point P lies between the y-coordinates of the two vertices that form one edge of the polygon.
ii) Point P is not a vertex point and is not above the boundary edges (this process is checked separately.)
iii) Add a cross number if the x-coordinate of the intersection point between the horizontal line (a straight line parallel to the x-axis) passes through point P and the edge is larger than the x-coordinate of point P.
iv) If the cross number is odd, point P is inside the polygon.

The result based on this process is information revealing whether the point P was located inside, outside, or above the boundary of the polygon. If the object contains a void space, the final location of the particle was determined using the Boolean operations on the outer polygon and inner void polygon. For example, if a point is located inside the outer polygon and outside the inner void polygon, we determine that the point is inside the object.

The meshfree analysis requires an appropriate normal vector for the particles located above the boundary. Among the normal vectors, a vector that faces outward from the 2D analysis domain is required in this study. The boundary shapes of the application model used here are a polygon or part of the circumference of a circle (an arc). The normal vector of the particle located on the arc was created by connecting the center of the arc to the particle. The normal vector of the particle located on the polygon was created using the following process (Fig. 11) based on the premise that the vertices of a polygon were created continuously in a constant direction. Here, the X'-axis is defined through
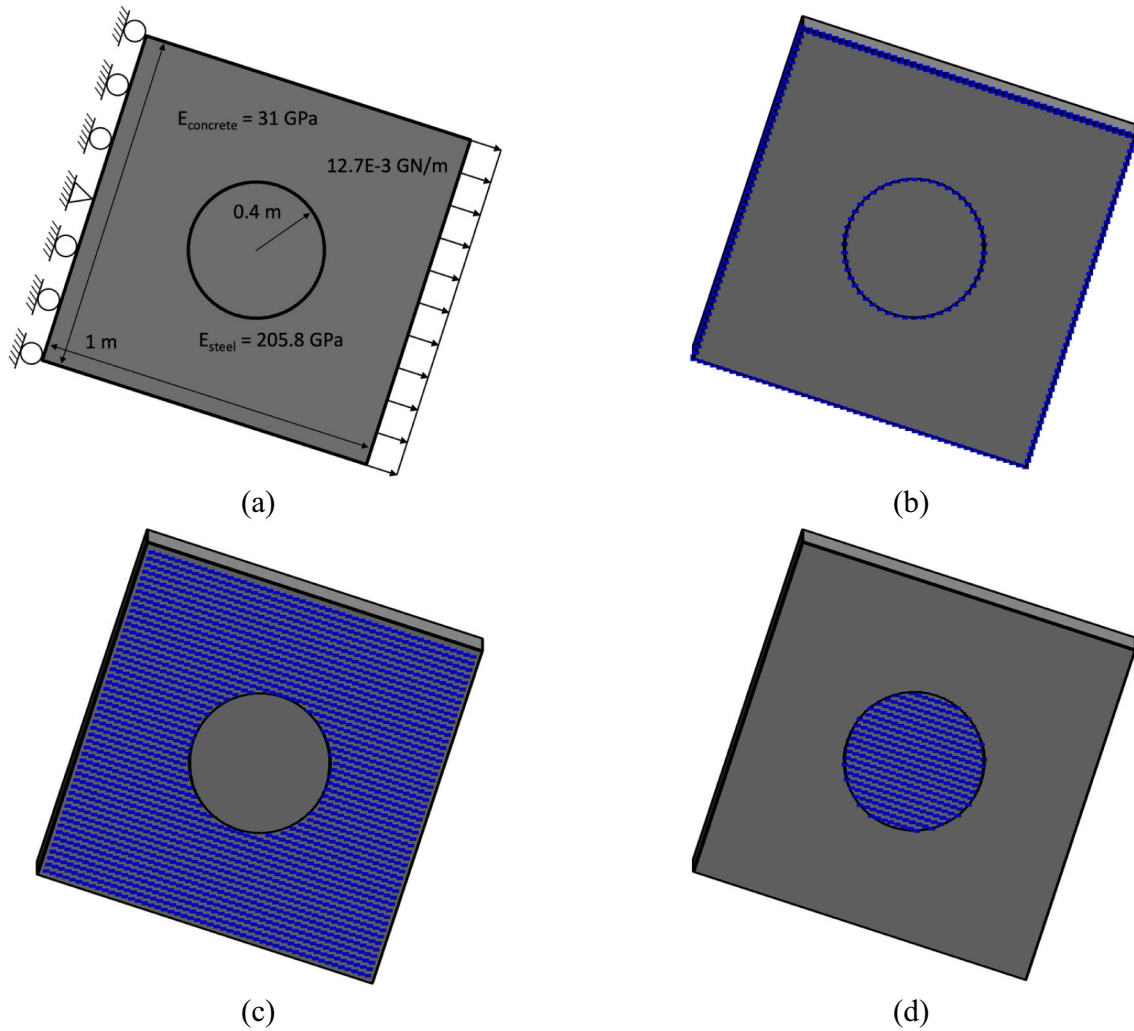
Fig. 12. Simple problem consisting of an object made of concrete and steel material to which the proposed analysis process is applied: (a), and analytical particles distributed in the analysis domain: (b) particles at the interface and (c), (d) particles in each sub-domain.

connecting the straight line with the next vertex (Pnext) based on one vertex (Po) and the Ytemp'-axis that connects to the previous vertex (Ppre) based on Po.

4.2.2. Analysis result information management via the meshfree method

As described above, in the meshfree analysis method, the displacements (the results of the analysis) are generated at the analytical particle points; the analysis results represent the displacement corresponding to the position of each particle, such that we can use the value to derive the stress and strain values of the particle. In this study, we used the following attributes: 1) the deformed geometry was represented using the particle position before analysis and the displacement values after analysis, 2) the displacement itself after analysis was used as the particle reactions, 3) the stress and strain derived from the displacement was linked to the particles using the newly defined IFC entities.

5. Experimental implementation of the IfcBridgeAddMeshfree-based numerical analysis

To confirm the possibility of IFC-based meshfree analysis and integrated information management, we applied the methodology proposed in this study to 1) a simple shaped object and 2) the diaphragm component of a steel bridge by mainly applying the FE analysis due to its complex shape. The 3D model was built using the module described

in Section 4.1. The generated model was used to extract the necessary information to perform numerical analysis, as well as to integrate the related information into the *IfcBridgeAddMeshfree*.

5.1. Simple object of the information model

Fig. 12(a) is the first example used to verify the applicability of the IFC-based meshfree analysis, which was built as a 3D object by extrusion based on a 2D profile with a square cross-section. The object comprises concrete material with a length and width of 1 m, with a circular steel inset that has a radius of 0.4 m in the center. We applied 31 GPa and 205.8 GPa, commonly used as Young's modulus, respectively. An external loading force of 12.7×10^{-3} GN/m was applied to the right side, the left side of the object was fixed by the rollers, and the center was only fixed by a pin.

The IFC-based information model was generated, including the conversion and extraction of the geometric and material information from the 3D model modeled using Autodesk Revit, as described in Section 4.1. This IPF is an initial IFC model that does not include external forces, boundary conditions, and meshfree particles. This is because the proposed process aims to integrate the analysis information based on the IFC. Therefore, analysis-related information was added later through the additional process. Table 2 lists a part of the initial IPF for the mentioned process, which was created according to the *IFC4Add2* and *IfcBridgeAddMeshfree* schemas.
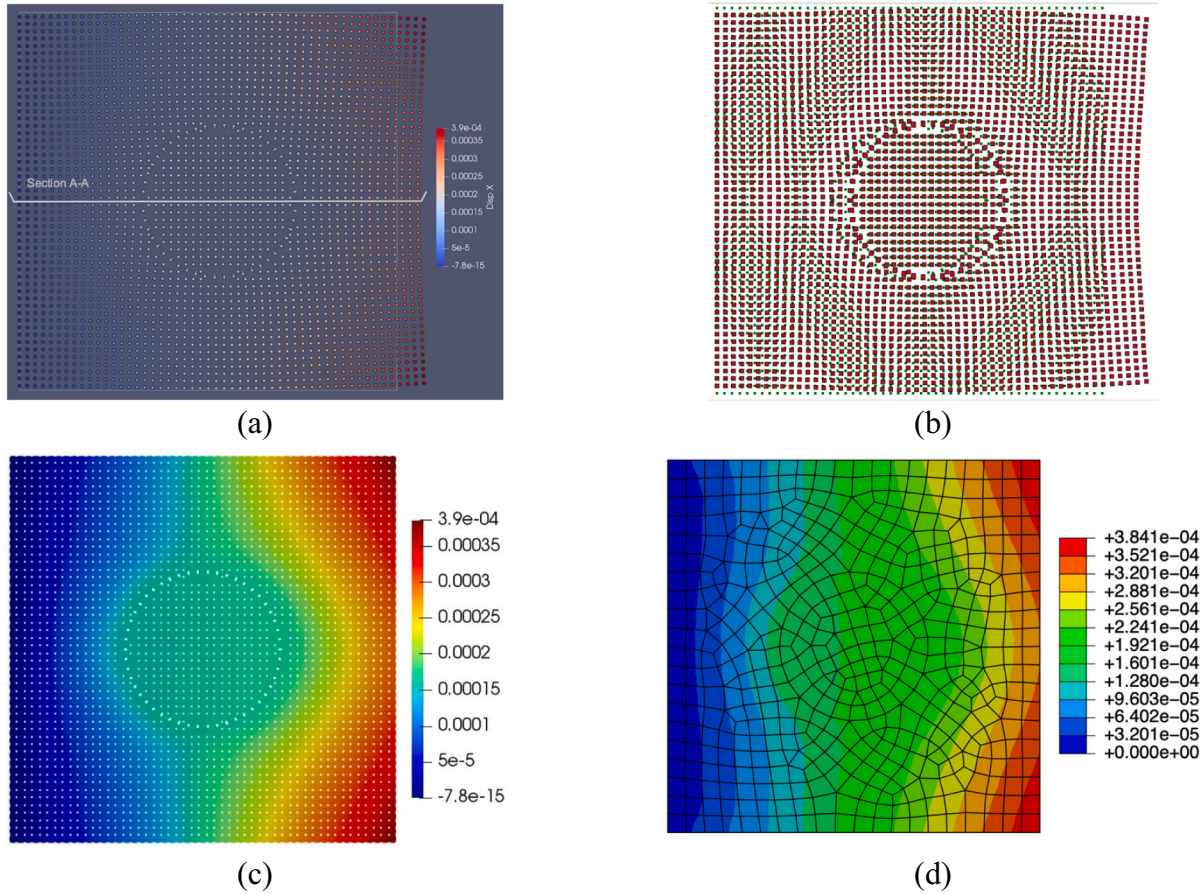
Fig. 13. Analysis results: (a) deformation, (b) deformation within the IPF, (c) contour map, and (d) the analysis results using Abaqus.

In Table 2, for the *IFC4Add2* schema, the two physical objects (i.e., the concrete and steel objects) were represented by the *IfcBuildingElementProxy* entities (#1297, #1298). These were connected with #1687 (*IfcBuildingStorey*) through #1660 (*IfcRelContainedInSpatialStructure*).

In contrast, these two objects can be represented as entities of the *IfcBridgeGirder* (#2328) and *IfcBridgeMember* (#1342) using the module shown in Fig. 10 for the *IfcBridgeAddMeshfree* schema-based model. These also contain basic functional information through the *PredefinedType* properties contained in both objects. Using #2314, the *IfcBridgeGirder* and *IfcBridgeMember* were connected to the *IfcBridge* (#1982). The "Geometry Info." Row (Table 2(b)) is the part that manages geometric information for the exterior concrete object. *IfcExtrudedAreaSolid* (#204) represented the geometry of the object, such that the cross section was implemented by #197 (*IfcArbitraryProfileDefWithVoids*) because of voids in the object. Among the attributes of *IfcArbitraryProfileDefWithVoids*, *OuterCurve* was represented by *IfcPolyline* (#178) while *InnerCurves* was implemented as *IfcCompositeCurve*, i.e., #193 by applying an internal void space. For the steel object, the cross section was represented by #192, where the detail entities were identical to #193. The "Material Info." row (See Table 2(c)) provides the material information. The *IfcMaterial* (#353) and *IfcMaterialProperties* (#379) entities were used for the material information. Here, #353 and the physical elements (#1342) of the *IfcBridgeAddMeshfree* were connected by the *IfcRelAssociatesMaterial* while #353 (*IfcMaterial*) was linked to the detailed information (#375, #376) through #379 (*IfcMaterialProperties*) as shown in Fig. 6. Fig. 12(b)–(d) shows the particles generated for the meshfree analysis based on the information extracted from the IPF.

Fig. 12(b) shows the particles for meshfree analysis at the interface, which contains information on the normal vector, as well as information on particle locations. As described above, the particles located at

the boundary surface were generated through a separate process. Fig. 12(c) and (d) are analytical particles scattered over the entire analysis plane, where we have used Process 1 to determine their locations.
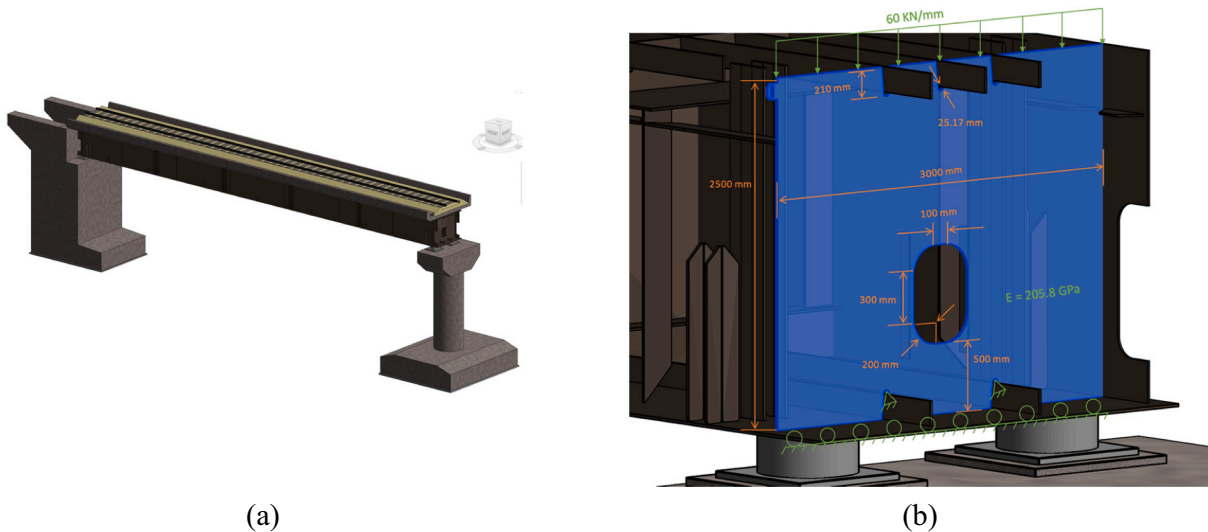
Fig. 13 shows the result of the analysis according to the above description. Fig. 13(a) visualizes the results of the displacements focused on particles derived from the meshfree analysis method proposed in this study using the ParaView tool [56]. These results can be integrated into the IPF. Fig. 13(b) shows the location of the particles before and after the analysis viewed with the FZKViewer [57], an IFC visualization tool. Table 3 lists the part of the IPF that includes Table 2 and their analysis results. At this time, the deformations show in Fig. 13(a) and (b) were exaggerated as compared with the actual deformation values for visualization. Fig. 13(c) and (d) show the contour plots for displacement based on the analysis. Fig. 13(c) is the result of applying the meshfree analysis method while Fig. 13(d) shows the analysis results based on the FE analysis method using the commercial software Abaqus [58] for comparison with Fig. 13(c). We can confirm that these two methods yielded identical results with negligible differences.

As shown in Fig. 7, the connection between the particle information and structural analysis model was through the *IfcRelAssignsToGroup*. The particles were represented using the *IfcStructuralPointConnection*, listed in #5352 of Table 3(a) for the IFC4-based model. As a result, we were able to confirm that *IfcCartesianPoint* (#3848) indicates the location of the particles based on local coordinates. The transformation of local coordinates is possible via #910, which is the instance of the *ObjectPlacement* attribute in the *IfcStructuralPointConnection* entity. The superordinate information for the structural analysis model was represented through *IfcStructuralAnalysisModel* (#762), which was connected through #761 (*IfcRelAssignsToGroup*). The actual values for the actions and reactions contained in the particles were represented by

Table 3
The part of the IPF including the analysis results.

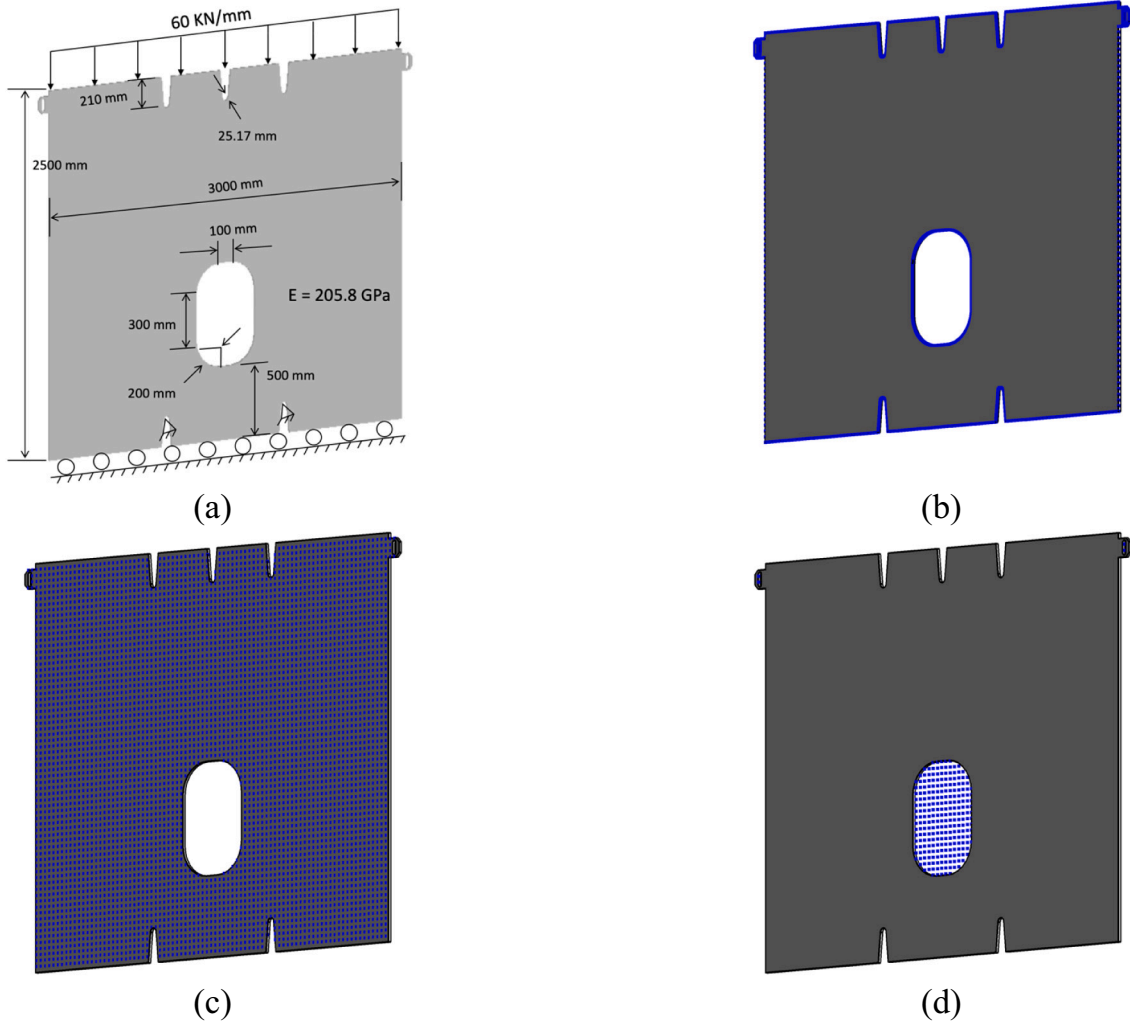| Schema	IFC physical file
(a) IFC4Add2	#761 = IFCRELASSIGNSTOGROUP('gxA7TejiR9aqK1wZ6IQylg',$,'Analysis - Connection',$,(#5274, …,#5352, …,#6024),.PRODUCT.,#762);
	#5352 = IFCSTRUCTURALPOINTCONNECTION('nVywnJPeRUSMWjUJA3KrZg',$,$,$,$,#910,#4599,$,$);
	#4599 = IFCPRODUCTDEFINITIONSHAPE($,$,(#6103));
	#6103 = IFCTOPOLOGYREPRESENTATION(#5272,'Reference','Vertex',(#2345));
	#2345 = IFCVERTEXPOINT(#3848);
	#3848 = IFCCARTESIANPOINT((1000.0,1000.0,0.0));
	#762 = IFCSTRUCTURALANALYSISMODEL('soX1HPvVQZW9/qfdjFWqcA',$,'Structural Analysis Model',$,$,.OUT_PLANE_LOADING_2D.,$,(#2265),(#7527),$);
	#2265 = IFCSTRUCTURALLOADCASE('NKXT/I6WR8umUnPYRKZvtQ',$,$,$,$,.LOAD_CASE.,.NOTDEFINED.,.DEAD_LOAD_G.,1.0,$,(0.0,0.0,0.0));
	#7527 = IFCSTRUCTURALRESULTGROUP('6kT5xe28R8WrGj3M5cQ06A',$,$,$,$,.USERDEFINED.,#2266,$);
	#2266 = IFCSTRUCTURALLOADCASE('gUZMbF + fSGiYLyykUcw06A',$,$,$,$,.LOAD_CASE.,.NOTDEFINED.,.DEAD_LOAD_G.,1.0,$,(0.0,0.0,0.0));
	#919 = IFCRELCONNECTSSTRUCTURALACTIVITY('qUn0MfP9RcCaqXEI6gspgA',$,'Member - Action',$,#5352,#7606);
	#7606 = IFCSTRUCTURALPOINTACTION('fEuaawwySq + RJwlqXC7KAA',$,'Point Action',$,$,$,$,#3096,.LOCAL_COORDS.,.F.);
	#3096 = IFCSTRUCTURALLOADSINGLEFORCE('Load',12.7E3,0.0,0.0,0.0,0.0,0.0);
	#920 = IFCRELCONNECTSSTRUCTURALACTIVITY('dL17a7jNRKSZ3ZnBQgnIHw',$,'Member - Reaction',$,#5352,#88);
	#88 = IFCSTRUCTURALPOINTREACTION('mHxZGTe1Q7qx6vxg3IcWig',$,'Point Reaction',$,$,$,$,#6854,.LOCAL_COORDS.);
	#6854 = IFCSTRUCTURALLOADSINGLEDISPLACEMENT('Displacement',3.85572E-4,-1.000117E-4,0,0.0,0.0,0.0);
(b) IfcBridgeAddMeshfree	#765 = IFCRELASSIGNSTOGROUP('Q1AAdxc5RSCMm98xwi9qUQ',$,'Analysis - Connection',$,(#2270, …,#2348, …,#3020),.PRODUCT.,#2269);
	#2348 = IFCSTRUCTURALPOINTMEMBER('dcT7URj3TOOXJrhRgYaZXg',$,$,$,$,#20110,#4601,.USERDEFINED.,#6103);
	#4601 = IFCPRODUCTDEFINITIONSHAPE($,$,(#1596));
	#1596 = IFCTOPOLOGYREPRESENTATION(#766,'Reference','Vertex',(#3099));
	#3099 = IFCVERTEXPOINT(#7606);
	#7606 = IFCCARTESIANPOINT((1000.0,1000.0,0.0));
	#6103 = IFCDIRECTION((0.7071068,0.7071068,0.0));
	#2269 = IFCSTRUCTURALANALYSISMODEL('BYipgZE0QQSSmK046QPSTw',$,'Structural Analysis Model',$,$,.OUT_PLANE_LOADING_2D.,$,(#762),$);
	#762 = IFCSTRUCTURALLOADCASE('e6lXQi7LQxexq + Tjno7wgw',$,$,$,$,.LOAD_CASE.,.NOTDEFINED.,.DEAD_LOAD_G.,1.0,$,(0.0,0.0,0.0));
	#710 = IFCSTRUCTURALRESULTGROUP('M2DH1EGmQZi72o9Oes4owQ',$,$,$,$,.USERDEFINED.,.MESHFREE_ANALYSIS_METHOD.,#763,$);
	#763 = IFCSTRUCTURALLOADCASE('KEA2fmYBQX2AZqDpRhScIA',$,$,$,$,.LOAD_CASE.,.NOTDEFINED.,.DEAD_LOAD_G.,1.0,$,(0.0,0.0,0.0));
	#10844 = IFCRELCONNECTSSTRUCTURALACTIVITY('MMasBVZrR6uqupNBP5xC/w',$,'Member - Action',$,#2348,#6854);
	#6854 = IFCSTRUCTURALPOINTACTION('82zE83jlRy + Fw55ZCIDFXA',$,'Point Action',$,$,$,$,#845,.LOCAL_COORDS.,.F.);
	#845 = IFCSTRUCTURALLOADSINGLEFORCE('Load',12.7E3,0.0,0.0,0.0,0.0,0.0);
	#10845 = IFCRELCONNECTSSTRUCTURALACTIVITY('o1jYGjS6TI + KG6L6aNiZxg',$,'Member - Reaction',$,#2348,#8513);
	#8513 = IFCSTRUCTURALPOINTREACTION('cWwzUK5fRlig + wi4k6uSlQ',$,'Point Reaction',$,$,$,$,#89,.LOCAL_COORDS.);
	#89 = IFCSTRUCTURALLOADSINGLEDISPLACEMENT('Displacement',3.85572E-4,-1.000117E-4,0.0,0.0,0.0,0.0);
	#10846 = IFCRELCONNECTSSTRUCTURALACTIVITY('q6ZWXrZ2Qoe5eG0XumFbDA',$,'Member - Stress',$,#2348,#8514);
	#8514 = IFCSTRUCTURALPOINTREACTION('8xqvcxJNT3Wq6Tu3ptHvfg',$,'Point Stress',$,$,$,$,#5352,.LOCAL_COORDS.);
	#5352 = IFCSTRUCTURALSINGLESTRESS('Stress',0.01582127,4.68203E-4,0.0,4.68203E-4,-0.001179362,0.0,0.0,0.0,0.0,0.0);
	#10847 = IFCRELCONNECTSSTRUCTURALACTIVITY('6BU8u2bKSbSaxhwDJn3W9w',$,'Member - Strain',$,#2348,#8515);
	#8515 = IFCSTRUCTURALPOINTREACTION('0JFa/W/ZQN2MxSRf76OtLw',$,'Point Strain',$,$,$,$,#3850,.LOCAL_COORDS.);
	#3850 = IFCSTRUCTURALSINGLESTRAIN('Strain',5.217768E-4,1.963432E-5,0.0,1.963432E-5,-1.91153E-4,0.0,0.0,0.0,0.0,0.0);

Fig. 14. Practical bridge component applied to the meshfree method process.

IfcStructuralPointAction and *IfcStructuralPointReaction*, which are subtypes of *IfcStructuralActivity*, listed in #7606 and #88 of Table 3(a), respectively. Table 3(a) lists the information for the top right point in Fig. 12, as shown in #3848. The loading condition of the point can be verified with #3096 (*IfcStructuralLoadSingleForce*), while the displacement analyzed using the meshfree method is contained in #6854 (*IfcStructuralLoadSingleDisplacement*). We also confirmed that the *IfcStructuralPointAction* and *IfcStructuralPointReaction* correctly connected

Table 4
Parts of the initial IPF, including the geometry and material information, generated using the developed IFC exporter module for the practical bridge model.

Schema	IFC4Add2	IfcBridgeAddMeshfree
(a) Spatial/ physical info.	#4571 = IFCRELAGGREGATES('1iD0mE7gQ0CLKO13HTJRqQ',#4578,'Bridge',$,#4565,(#4566)); #4572 = IFCRELAGGREGATES('PiFiacC2dEWb7Xdi/xEhvg',#4578,'SuperStructure',$,#4566,(#4567)); #4573 = IFCRELAGGREGATES('vvzsyNqPZU+pAHYmgRY7jQ',#4578,'Span2',$,#4567,(#4568)); #915 = IFCRELCONTAINEDINSPATIALSTRUCTURE('g7xnk2IVOECGVxniqPx1pQ',#4578,'Section1',$,(#10),#4568); #4565 = IFCBUILDINGSTOREY('aLTkS3q24kGpMYwPDgkFhQ',$,'Bridge','','',$,$,'',$,0.0); #4566 = IFCBUILDINGSTOREY('zlQqzZXPBkewTOrJXbvZog',$,'SuperStructure','','',$,$,'',$,0.0); #4567 = IFCBUILDINGSTOREY('y24XeWlVkkuYz9m9 + bfJfg',$,'Span2','','',$,$,'',$,0.0); #4568 = IFCBUILDINGSTOREY('SauD9jFAn0WPrtvXAW08kw',$,'Section1','','',$,$,'',$,0.0); #10 = IFCBUILDINGELEMENTPROXY ('A0MW4Fz6vkqEH1SVzi9GLA',#4578,'Diaphragm','','',#4576,#4509,'',.NOTDEFINED.);	#4568 = IFCRELAGGREGATES('lKL361M270WL4FxanCml4Q',#4578,'Bridge',$,#4509,(#4572)); #4569 = IFCRELAGGREGATES('1b1ALvPHjEKgLpT1fE7E3Q',#4578,'SuperStructure',$,#4572,(#4573)); #4570 = IFCRELAGGREGATES('M4FZx/JqlKGp2tEzgn/HxQ',#4578,'Span2',$,#4573,(#4574)); #914 = IFCRELCONTAINEDINSPATIALSTRUCTURE('np9OiX + sJ06Givso8jiaig',#4578,'Section1',$,(#4507),#4574); #4509 = IFCBRIDGE('aLTkS3q24kGpMYwPDgkFhQ',$,'Bridge','','',$, $,'',COMPLEX,.GIRDER_BRIDGE.,.MAIN_SPAN_BRIDGE.); #4572 = IFCBRIDGESPACEPART('zlQqzZXPBkewTOrJXbvZog',$,'SuperStructure','','',$, $,'',COMPLEX,.RAILWAY.); #4573 = IFCBRIDGESPACEPART('y24XeWlVkkuYz9m9 + bfJfg',$,'Span2','','',$, $,'',COMPLEX,.RAILWAY.); #4574 = IFCBRIDGESPACEPART('SauD9jFAn0WPrtvXAW08kw',$,'Section1','','',$, $,'',COMPLEX,.RAILWAY.); #4507 = IFCBRIDGEMEMBER ('A0MW4Fz6vkqEH1SVzi9GLA',#4578,'15 × 150','','',#4576,#4510,'',.DIAPHRAGM.);
(b) Geometry info.	#906 = IFCEXTRUDEDAREASOLID(#901,#905,#20,16.000000000137); #901 = IFCARBITRARYPROFILEDEFWITHVOIDS(.AREA.,'Diaphragm',#721,(#819,#859,#895)); #721 = IFCCOMPOSITECURVE((#470,#477, ...,#713,#720),.F.); #470 = IFCCOMPOSITECURVESEGMENT(.CONTINUOUS.,.T.,#468); #468 = IFCPOLYLINE((#464,#466)); #464 = IFCCARTESIANPOINT((700.554625807074,-1500.)); #720 = IFCCOMPOSITECURVESEGMENT(.CONTINUOUS.,.T.,#718); #718 = IFCPOLYLINE((#714,#716)); #819 = IFCCOMPOSITECURVE((#766,#773, ...,#811,#818),.F.); #766 = IFCCOMPOSITECURVESEGMENT(.CONTINUOUS.,.F.,#763); #763 = IFCTRIMMEDCURVE(#762,(IFCPARAMETERVALUE(180.)),(IFCPARAMETERVALUE(269.99999999999)),.T.,.PARAMETER.); #762 = IFCCIRCLE(#761,200.); #859 = IFCCOMPOSITECURVE((#835,#843,#850,#858),.F.); #835 = IFCCOMPOSITECURVESEGMENT(.CONTINUOUS.,.T.,#833); #833 = IFCPOLYLINE((#829,#831)); #843 = IFCCOMPOSITECURVESEGMENT(.CONTINUOUS.,.F.,#840); #840 = IFCTRIMMEDCURVE(#839,(IFCPARAMETERVALUE(0.)),(IFCPARAMETERVALUE(180.)),.T.,.PARAMETER.); #895 = IFCCOMPOSITECURVE((#872,#879,#887,#894),.F.);	
(c) Material info.	#615 = IFCRELASSOCIATESMATERIAL('12k9jd90FVCKi53RfleF9',#4578,$,$,(#2540),#655); #655 = IFCMATERIAL('Steel_SM',$,'Steel'); #699 = IFCMATERIALPROPERTIES('MaterialFactors',$,(#681,#682),#655); #681 = IFCPROPERTYSINGLEVALUE('YoungModulus',$,IFCMODULUSOFELASTICITYMEASURE(205800.),$); #682 = IFCPROPERTYSINGLEVALUE('PoissonRatio',$,IFCMODULUSOFELASTICITYMEASURE(0.3),$);	

Fig. 15. Model dimensions and applied conditions: (a), and analytical particles in the analysis domain: (b) particles at the interface, (c) particles in the analytical domain, and (d) particles in the inner hole.

with #5352 through *IfcRelConnectsStructuralActivity* (#919, #920). Table 3(b) reflects the extended entities, from which we can observe that *IfcStructuralPointMember* (#2348) indicates information on the particle. Unlike the IFC4 case, the entity contained information on the direction vector for the particle, such as #6103 (*Ifcdirection*). Further-more, #710 (*IfcStructuralResultGroup*) in Table 3(b) represents the analysis result, including the analysis information (MESHFREE_ANAL-YSIS_METHOD), as well as #7527 in Table 3(a). The analysis results connected with *IfcRelConnectsStructuralActivity* contained not only the displacement but also the stress (#5352) and strain (#3850) in the *IfcBridgeAddMeshfree* schema unlike IFC4.

5.2. Practical object in the bridge information model

Fig. 14(a) shows a part of a model for Jenaecheon railway Bridge in Ulsan, Korea. This bridge is a steel box girder bridge superstructure type, with a total length of 200 m, composed of five spans of 40 m. In this study, the meshfree analysis method was applied to the diaphragm component, which has been mostly analyzed using the FEM due to the complexity of its shape (Fig. 14(b)). The diaphragm has a width of 3 m and a height of 2.5 m with a hole consisting of arcs and straight lines in the center. The loading condition was applied at a value of 60 KN/mm in the downward direction of the diaphragm. Young's modulus was used at 205.8 GPa. The lower part of the object was fixed by the rollers while only the part of the auxiliary member was constrained by the

pins, as shown in Fig. 14(b). The initial IFC model was generated in the same manner as described in Section 5.1. Table 4 lists part of the initial IPF of the diaphragm for application to the meshfree method.

For *IFC4Add2*, the physical object of the diaphragm was represented by *IfcBuildingElementProxy* (#10) and was identical to case 1. Here, #10 was connected with spatial information defined in the 'Bridge,' 'Superstructure,' 'Span 2,' and 'Section 1' entities, which are managed in #4565, #4566, #4567, and #4568 (*IfcBuildingStorey*). The hierarchical relations throughout this information can be confirmed through #4571, #4572, and #4573 (*IfcRelAggregates*). Even if the IPF was generated based on the *IfcBridgeAddMeshfree*, the basic form was nearly identical to that based on *IFC4Add2* but the spatial information can be correctly represented (#4509, #4572, #4573, #4574), such that it was possible to specify the physical element of the diaphragm (#4507). Table 4(b) lists the geometric information for the diaphragm, which was essen-tially implemented as *IfcExtrudedAreaSolid*, *IfcArbitrar-yProfileDefWithVoids*, and *IfcCompositeCurve*, similar to Case 1. The material information was also generated in the same manner as in Case 1.

Fig. 15 shows the particles generated for the meshfree analysis based on the information extracted from the IPF. Similar to Fig. 12(b)–(d), Fig. 15(b) represents the particles used in the meshfree analysis at the interface, which include information on the normal vector, as well as the particles' location information. Fig. 15(c) shows the analytical particles scattered over the entire analytical domain.
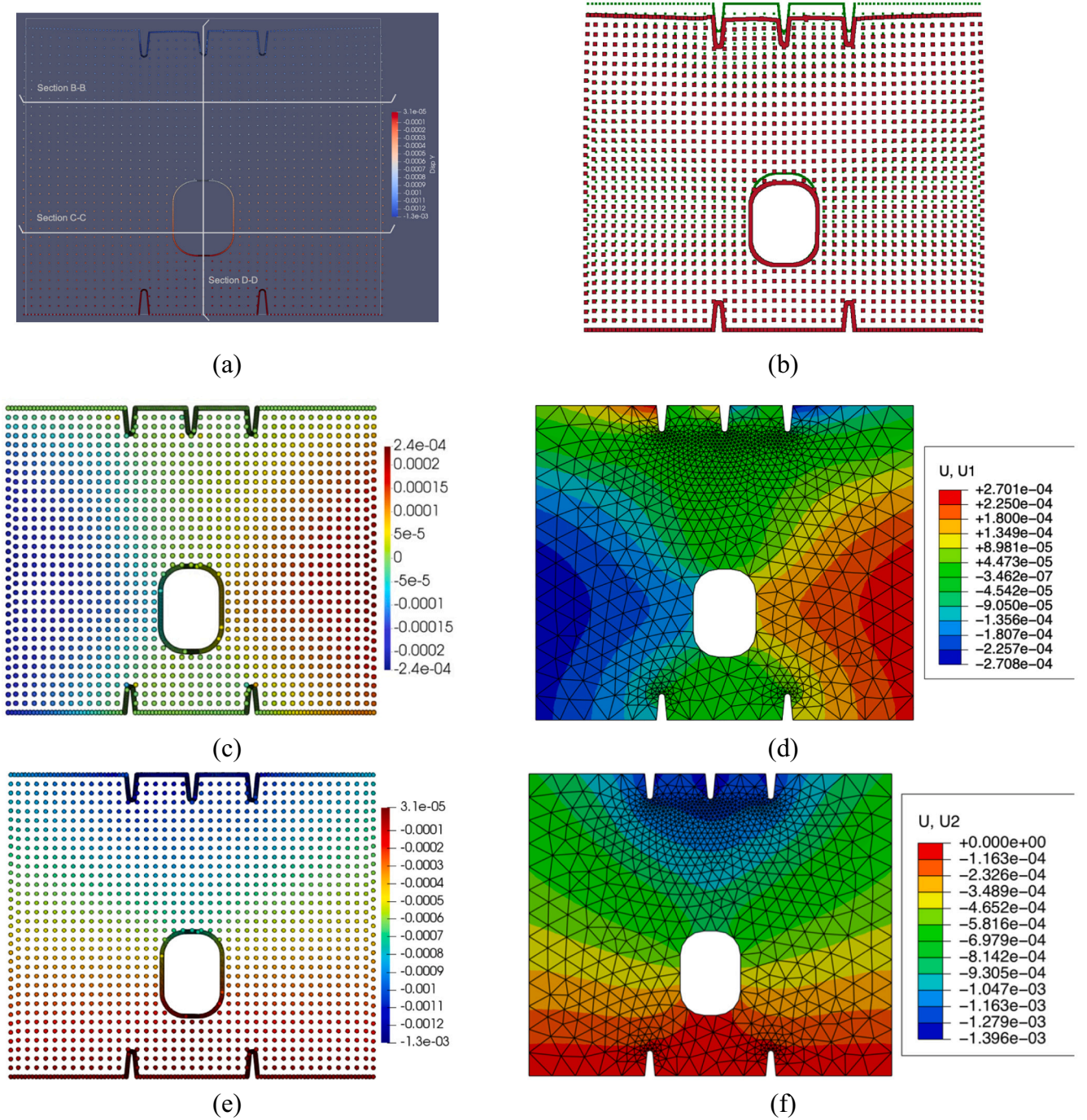
Fig. 16. Analysis results using the external conditions and generated particles: (a) Deformation, (b) deformation represented in the IPF, (c) the analysis result of displacement for the X-direction, (d) the analysis result based on Abaqus for the X-direction, (e) the analysis result of displacement for the Y-direction, and (f) the analysis result based on Abaqus for the Y-direction.

Particles located in the inner hole were automatically identified by applying the method proposed in this study as described in Section 5.2. Fig. 16 shows the analysis results using the external conditions and generated particles. Fig. 16(a) and (b) were also exaggerated for visualization as compared with the actual deformation values. Table 5 lists a part of the IPF regarding the analytical results, including basic information and external conditions.

The connection between the particle information and structural analysis model can be made through the *IfcRelAssignsToGroup*. The particle information was managed using *IfcStructuralPointConnection*, shown in #5029 in Table 5(a) for the IFC4-based model. The loading

condition was represented by *IfcStructuralLoadSingleForce* (#11655), which had displacement (#9447) as the reaction. The subtypes of *IfcStructuralActivity* represented the actual values for the actions and reactions contained by the particles, which were managed using *IfcStructuralPointAction* and *IfcStructuralPointReaction*, respectively, as shown in Fig. 8. We were able to check the values in #7238 and #16074 in Table 5(a). They were correctly connected to #5029 via *IfcRelConnectsStructuralActivity* (#21094, #21095). Table 5(b) lists the part of the IPF that reflects the *IfcBridgeAddMeshfree* schema. The analytical particles were represented using the *IfcStructuralPointMember* (#33739) entity. We were able to confirm that the analytical results

Table 5
The part of the IPF including the analysis results.

Schema	IFC physical file
(a) IFC4Add2	#6635 = IFCRELASSIGNSTOGROUP('nt5CdfNhRzuTdQX + VyrdOQ',$,'Analysis - Connection',$,(#4427, ...,#5029, ...,#6634),.PRODUCT.,#13261); #5029 = IFCSTRUCTURALPOINTCONNECTION('GipscxOgSgGJTAeFJJ2uSQ',$,$,$,$,$,#18282,$,$); #18282 = IFCPRODUCTDEFINITIONSHAPE($,$,(#2821)); #2821 = IFCTOPOLOGYREPRESENTATION(#8844,'Reference','Vertex',(#13864)); #13864 = IFCVERTEXPOINT(#613); #613 = IFCCARTESIANPOINT((2.242746E-12,2415.66467,0.0)); #13261 = IFCSTRUCTURALANALYSISMODEL('e9zU62mSRsemz2VNCLGc6g',$,'Structural Analysis Model',$,$,.OUT_PLANE_LOADING_2D.,$,(#15470),(#19888),$); #15470 = IFCSTRUCTURALLOADCASE('UxBX4PmpQ6WgfVoV88L + vQ',$,$,$,$,.LOAD_CASE.,.NOTDEFINED.,.DEAD_LOAD_G.,1.0,$,(0.0,0.0,0.0)); #19888 = IFCSTRUCTURALRESULTGROUP('qKuWgk0lTpG09KIU6vJQAQ',$,$,$,$,.USERDEFINED.,#15471,$); #15471 = IFCSTRUCTURALLOADCASE('f1DHHoz2QmixZQsvkbk5KA',$,$,$,$,.LOAD_CASE.,.NOTDEFINED.,.DEAD_LOAD_G.,1.0,$,(0.0,0.0,0.0)); #21094 = IFCRELCONNECTSSTRUCTURALACTIVITY('NgqlCluKTJyFz8rPhrSzWg',$,'Member - Action',$,#5029,#7238); #7238 = IFCSTRUCTURALPOINTACTION('sW6TT3x1STmvflp9ut39WQ',$,'Point Action',$,$,$,$,#11655,.LOCAL_COORDS.,.F.); #11655 = IFCSTRUCTURALLOADSINGLEFORCE('Load',0.0,-6.0E7,0.0,0.0,0.0,0.0); #21095 = IFCRELCONNECTSSTRUCTURALACTIVITY('gC3uszohTqGVMvaGKkmNjA',$,'Member - Reaction',$,#5029,#16074); #16074 = IFCSTRUCTURALPOINTREACTION('uOpOTmFDSHmVm9QAHiCTTw',$,'Point Reaction',$,$,$,$,#9447,.LOCAL_COORDS.); #9447 = IFCSTRUCTURALLOADSINGLEDISPLACEMENT('Displacement',2.242746E-17,-8.433533E-4,0.0,0.0,0.0,0.0);
(b) IfcBridgeAddMeshfree	#37553 = IFCRELASSIGNSTOGROUP('4 + IrDjy9QT + azOjQPjraMA',$,'Analysis - Connection',$,(#33137,...,#33739, ...,#35344),.PRODUCT.,#12); #33739 = IFCSTRUCTURALPOINTMEMBER('qjh9atT3RnGM6llAe4tPKA',$,$,$,$,$,#31529,.USERDEFINED.,#38156); #31529 = IFCPRODUCTDEFINITIONSHAPE($,$,(#22697)); #22697 = IFCTOPOLOGYREPRESENTATION(#13262,'Reference','Vertex',(#29321)); #29321 = IFCVERTEXPOINT(#11656); #11656 = IFCCARTESIANPOINT((2.242746E-12,2415.66467,0.0)); #38156 = IFCDIRECTION((-0.7071068,0.7071068,0.0)); #12 = IFCSTRUCTURALANALYSISMODEL('ei6A0CEpRhSCIJrRUztlTA',$,'Structural Analysis Model',$,$,.OUT_PLANE_LOADING_2D.,$,(#10),(#33135),$); #10 = IFCSTRUCTURALLOADCASE('1O7DeYE2Sf + JnIFHc427AQ',$,$,$,$,.LOAD_CASE.,.NOTDEFINED.,.DEAD_LOAD_G.,1.0,$,(0.0,0.0,0.0)); #33135 = IFCSTRUCTURALRESULTGROUP('h8YinK + RSD + jO2QPfO0A9Q',$,$,$,$,.USERDEFINED.,.MESHFREE_ANALYSIS_METHOD.,#11,$); #11 = IFCSTRUCTURALLOADCASE('PxL322UZT6uzFvIPTnYz6Q',$,$,$,$,.LOAD_CASE.,.NOTDEFINED.,.DEAD_LOAD_G.,1.0,$,(0.0,0.0,0.0)); #4629 = IFCRELCONNECTSSTRUCTURALACTIVITY('xTmPUASJQay4DAmhffytKA',$,'Member - Action',$,#33739,#24905); #24905 = IFCSTRUCTURALPOINTACTION('ustpLujYTSm48MHcG/M8Nw',$,'Point Action',$,$,$,$,#615,.LOCAL_COORDS.,.F.); #615 = IFCSTRUCTURALLOADSINGLEFORCE('Load',0.0,-6.0E7,0.0,0.0,0.0,0.0); #4630 = IFCRELCONNECTSSTRUCTURALACTIVITY('4lfd5lSUSKqeRljO5trMSg',$,'Member - Reaction',$,#33739,#15069); #15069 = IFCSTRUCTURALPOINTREACTION('IgpsrkekS5 + QXGpIZ/DP4g',$,'Point Reaction',$,$,$,$,#35947,.LOCAL_COORDS.); #35947 = IFCSTRUCTURALLOADSINGLEDISPLACEMENT('Displacement',2.242746E-17,-8.433533E-4,0.0,0.0,0.0,0.0); #4631 = IFCRELCONNECTSSTRUCTURALACTIVITY('R + cSqGOHTUqWLzgeYPIdbg',$,'Member - Stress',$,#33739,#15070); #15070 = IFCSTRUCTURALPOINTREACTION('fu + VgNtJRs+RODkoBneJCA',$,'Point Stress',$,$,$,$,#27113,.LOCAL_COORDS.); #27113 = IFCSTRUCTURALSINGLESTRESS('Stress',-0.01489307,0.009050057,0.0,0.009050057,-0.05781605,0.0,0.0,0.0,0.0); #4632 = IFCRELCONNECTSSTRUCTURALACTIVITY('LxHAS5 + NSxiQBD9DHLDczA',$,'Member - Strain',$,#33739,#15071); #15071 = IFCSTRUCTURALPOINTREACTION('AhAkKnRrTnKlyLypWmq4WA',$,'Point Strain',$,$,$,$,#20489,.LOCAL_COORDS.); #20489 = IFCSTRUCTURALSINGLESTRAIN('Strain',1.191324E-5,5.716751E-5,0.0,5.716751E-5,-2.592232E-4,0.0,0.0,0.0,0.0);

related to the particle, such as the load (#615), displacement (#35947), stress (#27113), and strain (#20489) can be managed based on the proposed schema (*IfcBridgeAddMeshfree*).

Although the strong-form-based meshfree analysis method applied to the information model in this study is a relatively recent method compared with general FE analysis, its accuracy has previously been verified in numerous studies. This study focused on the effective integration of the IFC-based information models and meshfree analysis methods. Accordingly, discussing the analytical results themselves is not within the scope of this study. The FE analysis, however, was performed using the Abaqus software as shown in Figs. 13(d), 16(d), and (f) to verify the validity of this process. Fig. 17 shows that the analysis results were reliable by comparing the displacement in the cross-sections based on the two analysis methods. While more rigorous validations of the integrated IFC-based computational analysis approach are required, it should be noted that each component, i.e., IFC model and numerical methods, has been separately validated within the similar context of the engineering problems [50].

6. Discussion and conclusions

As the meshfree method involves performance of the analysis using particles directly located in the domain, we can verify that the meshfree analysis method is a more straightforward process than the FE analysis.

The elements required for both analysis methods are identical in terms of the structural geometry, material properties, and external conditions (loading and boundary conditions). However, the meshfree method only requires particles located in the analysis domain and normal vectors in the boundary region, whereas the FEM required an additional mesh grid, as well as a complex post-process for indispensably linking nodes and analysis conditions or results.

Further research on improving the computational cost and linkage methods among the various applications can contribute to the spread of the proposed framework and diversification of the model integration. For example, FE analysis of components with complex shapes requiring B-splines or NURBS curves can be reduced the number of analysis nodes by using Isogeometric Analysis (IGA). It would work to advantages for the computational cost [59]. Approximate the solution of the PDE without the process of classical discretization using Artificial Neural Network (ANN) will be an excellent approach to linking various information models and analysis [60–62]. In particular, these methods can be expected effective interface/integration with IFC data in that they can deduce results only with data. The following approaches could derive more practical and advanced analytical results for the practical bridge structures; analytical interaction to consider material non-linearity that can occur in reinforced concrete members [63], application of data-driven solutions for efficient computation of multidimensional differential equations [60], and improvement of the numerical solution
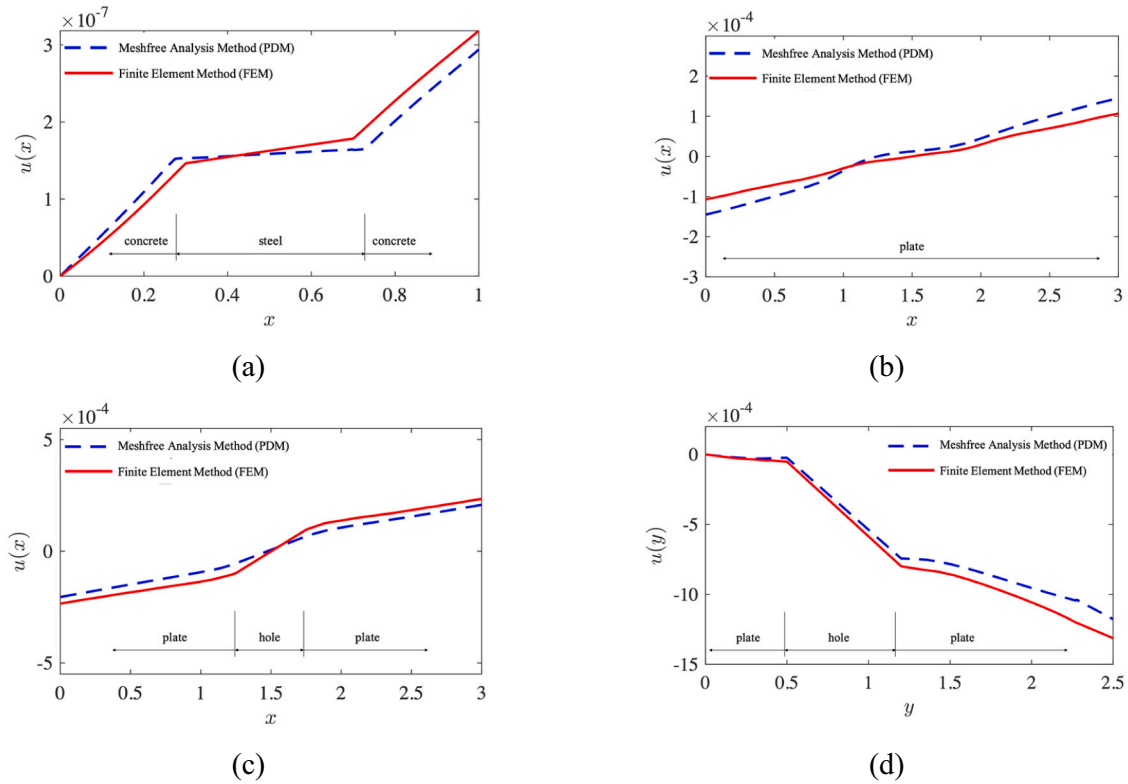
Fig. 17. Comparison of displacement based on the meshfree analysis method and FE analysis method for model sections: (a) section A-A for a simple case model (see Fig. 14(a)), (b) section B−B for a diaphragm model, (c) section C−C for a diaphragm model, and (d) section D-D for a diaphragm model (see Fig. 17(a)).

to track the influence of discretization in the process of initial information model-analysis-information integration with IFC [64].

The IFC data schema can support various ways of geometric modeling. These features are advantageous to model facilities with complex shapes. This, however, may produce possible information redundancy in terms of data processing. Therefore, we only used the extruded solid and B-rep based on a 3D geometric model perspective and limited to polygons and arcs, as well as circles in terms of the 2D profile. This is only an aspect of the geometry implementation and, therefore, does not affect the IFC-based usability review of the meshfree analysis.

In this study, we have chosen the bridge structure as the facility to apply the meshfree analysis method. This could be possible to check the extension and application of the IFC entities, as well as the meshfree analysis method. IFC extension for the bridge structures refers to results reported in previous studies. The *IFC4X2*, which is currently under development at buildingSMART, has entities for the bridge structure but this is not an official release and is therefore not included in this study. The prominent features of the *IFC4X2* compared with the previous IFC are the newly added *IfcFacility* and *IfcFacilityPart* as subtypes of the spatial element (*IfcSpatialStructureElement*). The entities for the building (*IfcBuilding*, *IfcBuildingStorey*) and bridge (*IfcBridge*, *IfcBridgePart*) facilities were added as subtypes of the *IfcFacility* and *IfcFacilityPart*. This approach in *IFC4X2* is more comprehensive than the proposed entities in this study. The proposed *IfcBridgeAddMeshfree* can then contribute to the concretization of the bridge component in the future. In particular, as this study follows the IFC extension concept, our method can be relatively easily integrated with existing IFC.

The extended IFC entities for the meshfree analysis, except for certain attributes, can be categorized as 1) the part that manages the particles as the analysis member (*IfcStructuralPointMember*) and 2) the part that controls the analysis results, such as stress and strain (*IfcStructuralSingleStress*, *IfcStructuralSingleStrain*). *IfcStructuralPointMember* is essential for the meshfree analysis. However, it may be necessary to reconsider the addition of these entities as *IfcStructuralSingleStress* and *IfcStructuralSingleStrain*

are derived through the post-process. However, we decided the addition of these entities for efficient re-analysis was more appropriate. Further expanding IFC model for different types of bridges and loading conditions remains as future work.

Contrary to the bright outlook and expectations for BIM, expansion into the application domain has been slow. This is in line with the difficulties associated with multidisciplinary collaboration that require not only an information model but also a high level of knowledge in the application field.

The FEM is essential for complex and detailed elements, or requires non-linear analysis. Intrinsically, however, the current IFC cannot support numerical analysis methods, such as FEM. Extrinsically, this is inefficient from an information management perspective; in the manual meshing process, where analysis result must be managed separately from input nodes, as well as remeshing process is required in situations that require re-analysis. The meshfree analysis method, especially the particle differential method used in this study, allow for numerical analysis without mesh generation. We note that the particle itself has input conditions and lead to analysis results. In this study, therefore, as one of the applications of the bridge information model, we proposed a meshfree analysis method process based on the IFC-based bridge model, examining its usability when combined with a practical bridge model. In this process, the current IFC was extended to support the bridge structure and meshfree analysis, and a module was developed to generate the information model. A process was presented to extract and process the data required for analysis and store the analysis results.

Except for the analytical particles, all the information required to apply meshfree analysis is included in the BIM model, rendering particle generation as a simple process due to the shape-independent feature. Recent studies have also confirmed the utility of meshfree analysis; the meshfree method is an analysis method that can be efficiently integrated with BIM. For example, there are numerous studies focused on generating BIM models [65–68] and connecting them with analyses that use cloud points acquired through laser scanning on existing

Table 2

Parts of the initial IPF, including the geometry and material information generated using the developed IFC exporter module.

Schema	IFC4Add2	IfcBridgeAddMeshfree
(a) Spatial/physical info.	#1660 = IFCRELCONTAINEDINSPATIA-LSTRUCTURE ('u7RNPHdB60qxrbN19PsQKg',#1661,'-Bridge',$,(#1297,#1298),#1687); #1687 = IFCBUILDINGSTOREY ('a + Zdk0rwxUivV4k2yUNtGw', $,'Bridge','','',$,$,'',$,0.0); #1297 = IFCBUILDINGELEMENTPROXY ('vcPWolgixUe	+5VyYZJtBNw',#1661,'concrete_1000_RV2016','','',#1303,#1688,'',.NOTDEFINED.); #1298 = IFCBUILDINGELEMENTPROXY ('jI3U9jPFIk + yQ4tuPvBXaA',#1661,'steel_r200_RV2016','','',#1303,#1689,'',.NOTDEFINED.);
#2314 = IFCRELCONTAI-NEDINSPATIALSTRUCT-URE ('fDuNwlZxSEqLLJWQry-pSbw',#1980,'Bridge',$, (#2328,#1342),#1982); #1982 = IFCBRIDGE ('a + Zdk0rwxUivV4k2y-UNtGw',$,'Bridge','','',$,		$,'',.ELEMENT.,.GIRDER_BRIDGE.,.MAIN_SPAN_BRIDGE.); #2328 = IFCBRIDGEGIRDER('vcPWolgixUe +5VyYZJtBNw',#1980,'concrete_1000_RV2016','','',#1981,#698,'',.CONCRETE_BOX_GIRDER.,$); #1342 = IFCBRIDGEMEMBER ('jI3U9jPFIk + yQ4tuPvBXaA',#1980,'steel_r200_RV2016','','',#1981,#699,'',.BAR.);
(b) Geometry info.	#204 = IFCEXTRUDEDAREASOLID(#197,#203,#20,250.); #197 = IFCARBITRARYPROFILEDEFWITHVOIDS(.AREA.,'concrete_1000_RV2016',#178,(#193)); #178 = IFCPOLYLINE((#170,#172,#174,#176,#170)); #170 = IFCCARTESIANPOINT((-500.,-500.)); #172 = IFCCARTESIANPOINT((500.,-500.)); #174 = IFCCARTESIANPOINT((500.,500.)); #176 = IFCCARTESIANPOINT((-500.,500.)); #193 = IFCCOMPOSITECURVE((#185,#192),.F.); #185 = IFCCOMPOSITECURVESEGMENT(.CONTINUOUS.,.F.,#182); #182 = IFCTRIMMEDCURVE(#181,(IFCPARAMETERVALUE(180.)),(IFCPARAMETERVALUE(3.56222124323914E-13)),.T.,.PARAMETER.); #181 = IFCCIRCLE(#180,200.); #180 = IFCAXIS2PLACEMENT2D(#10,#28); #192 = IFCCOMPOSITECURVESEGMENT(.CONTINUOUS.,.F.,#189);	
(c) Material Info.	#345 = IFCRELASSOCIATESMATERIAL('01kVXT9hb7C80NqRflZZF9',#209,$,$,(#2328),#353); #353 = IFCMATERIAL('concrete_RV2016',$,'Concrete'); #379 = IFCMATERIALPROPERTIES('MaterialFactors',$,(#375,#376),#353); #375 = IFCPROPERTYSINGLEVALUE('YoungModulus',$,IFCMODULUSOFELASTICITYMEASURE(31000.),$); #376 = IFCPROPERTYSINGLEVALUE('PoissonRatio',$,IFCMODULUSOFELASTICITYMEASURE(0.3),$);	

structures [14]. In this case, the cloud points can be directly used as analytical particles. Moreover, the results can be more acquired more rapidly and efficiently in terms of information management than performing FE analysis by generating meshes using cloud points. Our results show that we can reduce the overload when considering structural analysis in the process of building an architectural model. There should also be improvements in the interoperability of information throughout the life cycle of the structure.

Declaration of competing interest

The authors declare that they have no known competing financial interests or personal relationships that could have appeared to influence the work reported in this paper.

Acknowledgements

References

[1] J. Messner, C. Anumba, C. Dubler, S. Goodman, C. Kasprzak, R. Kreider, R. Leicht, C. Saluja, N. Zikic, BIM Project Execution Planning Guide, Version 2.2, Computer Integrated Construction Research Program, The Pennsylvania State University, 2019, https://www.bim.psu.edu/bim_pep_guide/4 , Accessed date: 22 June 2020.

[2] P. Sanguinetti, S. Abdelmohsen, J. Lee, J. Lee, H. Sheward, C.M. Eastman, General

system architecture for BIM: an integrated approach for design and analysis, Adv. Eng. Inform. 26 (2012) 317–333, https://doi.org/10.1016/j.aei.2011.12.001.

[3] Autodesk, Autodesk Robot Structural Analysis Professional 2021, https://help.autodesk.com/view/RSAPRO/2021/ENU/4, (2020) , Accessed date: 20 April 2020.

[4] Trimble Solutions Corporation, Tekla Structures 2019: Get started With Tekla Structures, https://teklastructures.support.tekla.com/tekla-structures-2019-pdf-documentation4, (2019) , Accessed date: 20 June 2020.

[5] Bentley Systems, Structural Enterprise: Structural Engineering Analysis and Design Software, https://www.bentley.com/en/resources/structural-enterprise4, (2019) , Accessed date: 20 June 2020.

[6] Allplan, Allplan Bridge: Modeling, Analysis and Detailing in a Single BIM Solution, https://www.allplan.com/us_en/products/bridge/4, (2020) , Accessed date: 20 June 2020.

[7] McGraw-Hill Construction, The Business Value of BIM for Construction in Major Global Markets: How Contractors Around the World are Driving Innovation With Building Information Modeling, https://www.construction.com/toolkit/reports/bim-business-value-construction-global-markets4, (2014) , Accessed date: 20 June 2020.

[8] L. Zhang, R.R.A. Issa, Ontology-based partial building information model extraction, J. Comput. Civ. Eng. 27 (2013) 576–584, https://doi.org/10.1061/(ASCE)CP.1943-5487.0000277.

[9] I.J. Ramaji, A.M. Memari, Interpreted information exchange: systematic approach for BIM to engineering analysis information transformations, J. Comput. Civ. Eng. 30 (2016) 04016028, , https://doi.org/10.1061/(ASCE)CP.1943-5487.0000591.

[10] R. Sacks, C.M. Eastman, G. Lee, P. Teicholz, BIM Handbook: A Guide to Building Information Modeling for Owners, Designers, Engineers, Contractors, and Facility Managers, 3rd ed., John Wiley & Sons, Inc., 9781119287544, 2018.

[11] M.F. Muller, A. Garbers, F. Esmanioto, N. Huber, E.R. Loures, O.J. Canciglieri, Data interoperability assessment though IFC for BIM in structural design–a five-year gap analysis, J. Civ. Eng. Manag. 23 (2017) 943–954, https://doi.org/10.3846/13923730.2017.1341850.

[12] I.J. Ramaji, A.M. Memari, Interpretation of structural analytical models from the coordination view in building information models, Autom. Constr. 90 (2018) 117–133, https://doi.org/10.1016/j.autcon.2018.02.025.

[13] R. Ren, J. Zhang, H.N. Dib, BIM Interoperability for Structure Analysis, Construction Research Congress 2018, New Orleans, Louisiana, USA, 2018, pp.

470–479. doi:https://doi.org/10.1061/9780784481264.046.

[14] L. Barazzetti, F. Banfi, R. Brumana, G. Gusmeroli, M. Previtali, G. Schiantarelli, Cloud-to-BIM-to-FEM: structural simulation with accurate historic BIM from laser scans, Simul. Model. Pract. Theory 57 (2015) 71–87, https://doi.org/10.1016/j.simpat.2015.06.004.

[15] buildingSMART International, Industry Foundation Classes Release 4X1 (IFC4x1) Final, https://standards.buildingsmart.org/IFC/RELEASE/IFC4_1/FINAL/HTML/4, (2018) , Accessed date: 15 February 2019.

[16] Solibri, Solibri Office, https://www.solibri.com/4, (2020) , Accessed date: 10 January 2020.

[17] N. Moës, J. Dolbow, T. Belytschko, A finite element method for crack growth without remeshing, Int. J. Numer. Methods Eng. 46 (1999) 131–150, https://doi.org/10.1002/(SICI)1097-0207(19990910)46:1<131::AID-NME726>3.0.CO;2-J.

[18] Y.-C. Yoon, J.-H. Song, Extended particle difference method for weak and strong discontinuity problems: part I. Derivation of the extended particle derivative approximation for the representation of weak and strong discontinuities, Comput. Mech. 53 (2014) 1087–1103, https://doi.org/10.1007/s00466-013-0950-8.

[19] T. Rabczuk, J.-H. Song, X. Zhuang, C. Anitescu, Extended Finite Element and Meshfree Methods, 1 ed., Academic Press, 978-0128141069, 2019.

[20] ISO-TC59/SC13, ISO 16739-1:2018 Industry Foundation Classes (IFC) for Data Sharing in the Construction and Facility Management Industries – Part 1: Data Schema, https://www.iso.org/standard/70303.html4, (2018) , Accessed date: 20 June 2020.

[21] ISO-TC184/SC4, ISO 10303-11: 2004 Industrial Automation Systems and Integration – Product Data Representation and Exchange – Part 11: Description Methods: The EXPRESS Language Reference Manual, https://www.iso.org/standard/38047.html4, (2004) , Accessed date: 20 June 2020.

[22] C.M. Eastman, P. Teicholz, R. Sacks, K. Liston, BIM Handbook: A Guide to Building Information Modeling for Owners, Managers, Designers, Engineers, and Contractors, 1st ed., John Wiley and Sons, Hoboken, NJ, 0470185287, 2008.

[23] J. Wix, J. Karlshøj, Information Delivery Manual Ver 1.2- Guide to Components and Development Methods, buildingSMART International, 2010, https://standards.buildingsmart.org/documents/IDM/IDM_guide-CompsAndDevMethods-IDMC_004-v1_2.pdf4 , Accessed date: 20 June 2020.

[24] buildingSMART International, Open standards - the basics, https://www.buildingsmart.org/standards/technical-vision/open-standards/4, (2019) , Accessed date: 10 March 2019.

[25] buildingSMART International, Model View Definition Summary, https://technical.buildingsmart.org/standards/mvd/mvd-database/4, (2019) , Accessed date: 10 October 2019.

[26] R. See, IFC Solutions Factory - The Model View Definition Site, http://www.blis-project.org/IAI-MVD/4, (2019) , Accessed date: 10 March 2019.

[27] S. Lehtinen, J. Hietanen, Generic AEC/FM View Description - Structural Design to Structural Analysis Ver 1.0, Virtual Building Laboratory, Tampere University of Technology, 2007, http://www.blis-project.org/IAI-MVD/4 , Accessed date: 21 June 2020.

[28] S. Lehtinen, Generic AEC/FM View Description - Architectural Design to Structural Design Ver 3, Virtual Building Laboratory, Tampere University of Technology, 2009, http://www.blis-project.org/IAI-MVD/4 , Accessed date: 21 June 2020.

[29] M. Weise, P. Katranuschkov, T. Liebich, R.J. Scherer, Structural analysis extension of the IFC modelling framework, Journal of Information Technology in Construction (ITcon) 8 (2003) 181–200 http://www.itcon.org/2003/14.

[30] A. Yasaka, H. Kataoka, K. Kasima, M. Takeda, M. Usami, N. Yabuki, N. Matumoto, S. Furukawa, Y. Mogi, Y. Adachi, The development of the reinforced-concrete structural model on IFC specification, Joint International Conference on Computing and Decision Making in Civil and Building Engineering, June 14-16, Montréal, Canada, 2006, pp. 3116–3125 https://architektur-informatik.scix.net/pdfs/w78-2006-tf487.pdf.

[31] Z.-Z. Hu, X.-Y. Zhang, H.-W. Wang, M. Kassem, Improving interoperability between architectural and structural design models: an industry foundation classes-based approach with web-based tools, Autom. Constr. 66 (2016) 29–42, https://doi.org/10.1016/j.autcon.2016.02.001.

[32] Z.-Q. Liu, F. Zhang, J. Zhang, The building information modeling and its use for data transformation in the structural design stage, Journal of Applied Science and Engineering 19 (2016) 273–284, https://doi.org/10.6180/jase.2016.19.3.05.

[33] L. Qin, X.-y. Deng, X.-l. Liu, Industry foundation classes based integration of architectural design and structural analysis, Journal of Shanghai Jiaotong University (Science) 16 (2011) 83–90, https://doi.org/10.1007/s12204-011-1099-2.

[34] R. Pukl, P. Pálek, J. Červenka, The possibility of using BIM for nonlinear life-cycle analysis of concrete structures, The Fifth International Symposium on Life-Cycle Civil Engineering (IALCCE 2016), Oct. 16–20, Delft, Netherlands, 2016, pp. 655–661 https://www.semanticscholar.org/paper/The-possibility-of-using-BIM-for-nonlinear-analysis-Pukl-P%C3%A1lek/fa2ab8e78ea5de8e07d5e94383f207ea0e669d95.

[35] J. Ninić, C. Koch, J. Stascheit, An integrated platform for design and numerical analysis of shield tunnelling processes on different levels of detail, Adv. Eng. Softw. 112 (2017) 165–179, https://doi.org/10.1016/j.advengsoft.2017.05.012.

[36] Autodesk, Revit, https://www.autodesk.com/products/revit/overview4, (2020) , Accessed date: 11 January 2020.

[37] Y.-C. Yoon, J.-H. Song, Extended particle difference method for weak and strong discontinuity problems: part II. Formulations and applications for various interfacial singularity problems, Comput. Mech. 53 (2014) 1105–1128, https://doi.org/10.1007/s00466-013-0951-7.

[38] Y.-C. Yoon, J.-H. Song, Extended particle difference method for moving boundary problems, Comput. Mech. 54 (2014) 723–743, https://doi.org/10.1007/s00466-014-1029-x.

[39] Y. Fu, J.G. Michopoulos, J.-H. Song, Bridging the multi phase-field and molecular dynamics models for the solidification of nano-crystals, J. Comput. Sci. 20 (2017) 187–197, https://doi.org/10.1016/j.jocs.2016.10.014.

[40] J.-H. Song, Y. Fu, T.-Y. Kim, Y.-C. Yoon, J.G. Michopoulos, T. Rabczuk, Phase field simulations of coupled microstructure solidification problems via the strong form particle difference method, Int. J. Mech. Mater. Des. 14 (2018) 491–509, https://doi.org/10.1007/s10999-017-9386-1.

[41] A. Almasi, A. Beel, T.-Y. Kim, J.G. Michopoulos, J.-H. Song, Strong-form collocation method for solidification and mechanical analysis of polycrystalline materials, J. Eng. Mech. 145 (2019) 04019082, , https://doi.org/10.1061/(asce)em.1943-7889.0001665.

[42] Y.-C. Yoon, P. Schaefferkoetter, T. Rabczuk, J.-H. Song, New strong formulation for material nonlinear problems based on the particle difference method, Engineering Analysis with Boundary Elements 98 (2019) 310–327, https://doi.org/10.1016/j.enganabound.2018.10.015.

[43] A. Beel, T.-Y. Kim, W. Jiang, J.-H. Song, Strong form-based meshfree collocation method for wind-driven ocean circulation, Comput. Methods Appl. Mech. 351 (2019) 404–421, https://doi.org/10.1016/j.cma.2019.03.045.

[44] A. Almasi, T.-Y. Kim, T.A. Laursen, J.-H. Song, A strong form meshfree collocation method for frictional contact on a rigid obstacle, Comput. Methods Appl. Mech. Eng. 357 (2019) 112597, https://doi.org/10.1016/j.cma.2019.112597.

[45] S.-H. Lee, K.-H. Kim, Y.-C. Yoon, Particle difference method for dynamic crack propagation, International Journal of Impact Engineering 87 (2016) 132–145, https://doi.org/10.1016/j.ijimpeng.2015.06.001.

[46] S.-H. Lee, B.-G. Kim, S.I. Park, Integration of bridge model data and engineering document information, The 30th CIB W78 International Conference, Oct. 9–12, Beijing, China, 2013, pp. 632–641 https://www.semanticscholar.org/paper/INTEGRATION-OF-BRIDGE-MODEL-DATA-AND-ENGINEERING-Lee-Kim/0b3cfc81080ae0c43bcd99826a9fd76bef38114f?citationIntent=background#citing-papers.

[47] G. Lee, C.M. Eastman, R. Sacks, S.B. Navathe, Grammatical rules for specifying information for automated product data modeling, Adv. Eng. Inform. 20 (2006) 155–170, https://doi.org/10.1016/j.aei.2005.08.003.

[48] S.-H. Lee, B.-G. Kim, IFC extension for road structures and digital modeling, Procedia Engineering 14 (2011) 1037–1042, https://doi.org/10.1016/j.proeng.2011.07.130.

[49] China Railway BIM Alliance (CRBIM), Railway BIM Data Standard Version 1.0, China Railway BIM Alliance, 2015, https://www.buildingsmart.org/wp-content/uploads/2017/09/bSI-SPEC-Rail.pdf4 , Accessed date: 18 June 2020.

[50] S.I. Park, J. Park, B.-G. Kim, S.-H. Lee, Improving applicability for information model of an IFC-based steel bridge in the design phase using functional meanings of bridge components, Appl. Sci. 8 (2018) 2531, https://doi.org/10.3390/app8122531.

[51] buildingSMART International MSG, Industry Foundation Classes 4 (IFC4) Addendum 2, http://www.buildingsmart-tech.org/specifications/ifc-releases/ifc4-add24, (2016) , Accessed date: 10 February 2019.

[52] STEP Tools Software, ST-Developer Tools Reference Manual, STEP Tools, Inc., 2010, https://www.steptools.com/support/4 , Accessed date: 18 June 2020.

[53] J. Frijters, IKVM.NET, https://www.ikvm.net/4, (2017) , Accessed date: 21 August 2017.

[54] T. Akenine-Möller, E. Haines, N. Hoffman, A. Pesce, M. Iwanicki, S. Hillaire, Real-Time Rendering, 4th ed., CRC Press, 978-1138627000, 2018.

[55] D. Sunday, Inclusion of a point in a polygon, http://geomalgorithms.com/a03-_inclusion.html4, (2019) , Accessed date: 10 March 2019.

[56] Kitware, ParaView, https://www.kitware.com/4, (2019) , Accessed date: 11 November 2019.

[57] Karlsruhe Institute of Technology, FZKViewer, https://www.iai.kit.edu/english/1648.php4, (2020) , Accessed date: 5 February 2020.

[58] Dassault Systemes, Abaqus Unified FEA, https://www.3ds.com/products-services/simulia/products/abaqus/4, (2020) , Accessed date: 18 February 2020.

[59] T.J.R. Hughes, J.A. Cottrell, Y. Bazilevs, Isogeometric analysis: CAD, finite elements, NURBS, exact geometry and mesh refinement, Comput. Methods Appl. Mech. Eng. 194 (2005) 4135–4195, https://doi.org/10.1016/j.cma.2004.10.008.

[60] C. Anitescu, E. Atroshchenko, N. Alajlan, T. Rabczuk, Artificial neural network methods for the solution of second order boundary value problems, Computers, Materials & Continua 59 (2019) 345–359, https://doi.org/10.32604/cmc.2019.06641.

[61] H. Guo, X. Zhuang, T. Rabczuk, A deep collocation method for the bending analysis of kirchhoff plate, Computers, Materials & Continua 59 (2019) 433–456, https://doi.org/10.32604/cmc.2019.06660.

[62] E. Samaniego, C. Anitescu, S. Goswami, V.M. Nguyen-Thanh, H. Guo, K. Hamdia, T. Rabczuk, X. Zhuang, An energy approach to the solution of partial differential equations in computational mechanics via machine learning: concepts, implementation and applications, Comput. Methods Appl. Mech. Eng. 362 (2020) 112790, https://doi.org/10.1016/j.cma.2019.112790.

[63] T. Rabczuk, G. Zi, S. Bordas, H. Nguyen-Xuan, A geometrically non-linear three-dimensional cohesive crack method for reinforced concrete structures, Eng. Fract. Mech. 75 (2008) 4740–4758, https://doi.org/10.1016/j.engfracmech.2008.06.019.

[64] N. Vu-Bac, T. Lahmer, X. Zhuang, T. Nguyen-Thoi, T. Rabczuk, A software framework for probabilistic sensitivity analysis for computationally expensive models, Adv. Eng. Softw. 100 (2016) 19–31, https://doi.org/10.1016/j.advengsoft.2016.06.005.

[65] H. Macher, T. Landes, P. Grussenmeyer, From point clouds to building information models: 3D semi-automatic reconstruction of indoors of existing buildings, Applied Sciences (Switzerland) 7 (2017), https://doi.org/10.3390/app7101030.

[66] F. Bosché, M. Ahmed, Y. Turkan, C.T. Haas, R. Haas, The value of integrating Scan-

to-BIM and Scan-vs-BIM techniques for construction monitoring using laser scanning and BIM: the case of cylindrical MEP components, Autom. Constr. 49 (2015) 201–213, https://doi.org/10.1016/j.autcon.2014.05.014.

[67] X. Xiong, A. Adan, B. Akinci, D. Huber, Automatic creation of semantically rich 3D building models from laser scanner data, Autom. Constr. 31 (2013) 325–337, https://doi.org/10.1016/j.autcon.2012.10.006.

[68] P. Tang, D. Huber, B. Akinci, R. Lipman, A. Lytle, Automatic reconstruction of as-built building information models from laser-scanned point clouds: a review of related techniques, Autom. Constr. 19 (2010) 829–843, https://doi.org/10.1016/j.autcon.2010.06.007.